Critical review on improved electrochemical impedance spectroscopy-cuckoo search-Elman neural network modeling methods for whole-life-cycle health state estimation of lithium-ion battery energy storage systems.

XIONG, R., WANG, S., TAKYI-ANINAKWA, P., JIN, S., FERNANDEZ, C., HUANG, Q., HU, W. and ZHAN, W.

2024

Critical Review on Improved Electrochemical Impedance Spectroscopy-cuckoo Search-Elman Neural Network Modeling Methods for Whole-life-cycle Health State Estimation of Lithium-ion Battery Energy Storage Systems

Ran Xiong, Shunli Wang, Paul Takyi-Aninakwa, Siyu Jin, *Member, IEEE*, Carlos Fernandez, Qi Huang, *Fellow*, *IEEE*, Weihao Hu, *Senior Member*, *IEEE*, Wei Zhan

***Abstract*—Efficient and accurate health state estimation is crucial for lithium-ion battery (LIB) performance monitoring and economic evaluation. Effectively estimating the health state of LIBs online is the key but is also the most difficult task for energy storage systems. With high adaptability and applicability advantages, battery health state estimation based on data-driven techniques has attracted extensive attention from researchers around the world. Artificial neural network (ANN)-based methods are often used for state estimations of LIBs. As one of the ANN methods, the Elman neural network (ENN) model has been improved to estimate the battery state more efficiently and accurately. In this paper, an improved ENN estimation method based on electrochemical impedance spectroscopy (EIS) and cuckoo search (CS) is established as the EIS-CS-ENN model to estimate the health state of LIBs. Also, the paper conducts a critical review of various ANN models against the EIS-CS-ENN model. This demonstrates that the EIS-CS-ENN model outperforms other models. The review also proves that, under the same conditions, selecting appropriate health indicators (HIs) according to the mathematical modeling ability and state requirements are the keys in estimating the health state efficiently. In the calculation process, several evaluation indicators are adopted to analyze and compare the modeling accuracy with other existing methods. Through the analysis of the evaluation results and the selection of HIs, conclusions and suggestions are put forward. Also, the robustness of the EIS-CS-ENN model for the health state estimation of LIBs is verified.**

***Index Terms*—Lithium-ion battery, health state estimation, elman neural network, electrochemical impedance spectroscopy, cuckoo search, health indicators.**

I. Introduction

The remarkable attributes of high energy density, prolonged cycle life, and satisfactory performance have positioned lithium-ion batteries (LIBs) as the increasingly prevalent components in electric and energy storage systems [1]. As an essential part of and key equipment for energy storage, the capacity of LIBs degrades along with their continuous application. This leads to the overall whole-life-cycle health state decline. With the continuous optimization and improvement of internal materials as well as the rapid development of working performance, LIBs are also widely used in portable electronic products, aerospace, pure electric vehicles, energy storage power stations, and other fields using new energy [2].

Because of the complexity of energy systems, energy storage assumes a dual role as a critical technology and fundamental apparatus in the establishment of novel power systems, while simultaneously facilitating endeavors towards achieving carbon neutrality [3]. Conventional energy storage methods primarily encompass mechanical and electrochemical systems [4], [5]. The clean energy research community has shown significant interest in the field of energy storage systems because they can provide peak regulation, frequency modulation, backup, black start, demand response support, and other services [6], [7]. In [8], fast-response energy storage technologies are used for frequency regulation of modern power systems. In energy storage power stations, especially in large-scale photovoltaic energy stations, electrochemical energy storage technology has witnessed significant adoption and has become the principal foundation for reliable support [9], [10]. As the key equip-

Received: March 29, 2023
Accepted: December 11, 2023
Published Online: March 1, 2024
Shunli Wang (corresponding author) is with the School of Information Engineering, Southwest University of Science and Technology, Mianyang, 621010 China (e-mail: wangshunli@swust.edu.cn).
DOI: 10.23919/PCMP.2023.000234

ment of energy storage systems, the safety and performance of LIBs are essential to ensure the optimal operation of energy storage power stations [11], [12]. Inappropriate battery health management may lead to a series of issues, including fast aging and capacity degradation, module failure, thermal runaway, fire, explosions, etc., because of the rapid electrochemical reactions [6], [9], [13]. Thus, the establishment of an efficient and high-precision battery management system (BMS) serves as the cornerstone for ensuring the safety and dependability of contemporary energy storage systems. The application of LIBs in diverse conditions also holds considerable engineering value [14]. Their safety and stability are as important as their efficiency [15]. Therefore, efficient and accurate health state estimation is essential to ensure system and personal safety [16], [17]. It not only optimizes energy management strategies but also reflects the economic value of LIBs [18]–[21].

Many health state estimation methods for LIBs have a variety of shortcomings. There is a need to enhance the existing estimation methods and verify the engineering applicability of the optimized methods [22]. Because of the strong nonlinear characteristics of LIBs, it is a challenge to reasonably estimate the health state in stable conditions. Some methods have had some success in various fields. The techniques are categorized into two main groups: direct measurement and indirect analysis methods. These include physical model-based, data-driven, and hybrid methods.

The direct measurement methods include Coulomb counting and electrochemical impedance spectroscopy (EIS). These are not suitable for real-time application because their accuracy mainly depends on the battery state and the ambient operating conditions [23]. The physical model-based methods estimate the health state by establishing an equivalent circuit model (ECM) or an electrochemical model (EM) to combine various filters, including the extended Kalman filter (EKF), unscented Kalman filter (UKF), cubature Kalman filter (CKF), particle filter (PF), and H-infinity [24], [25]. In contrast to physical model-based methods, the data-driven methods obtain their result by constructing a black box model by extracting relevant information related to the health state.

Machine learning (ML)-based data-driven methods, such as the support vector machine (SVM), the relevance vector machine (RVM), fuzzy logic (FL), artificial neural network (ANN), etc., are often used as models to predict and estimate battery states [19], [26]–[29]. The accuracy of estimation results is contingent upon the ability of the network in selecting the health indicators (HIs) and corresponding operations. In addition, for LIBs, there is a special data-driven method called differential analysis (DA) to estimate their health state. This includes incremental capacity analysis (ICA) and differential voltage analysis (DVA) [30]. Each hybrid method combines one or more of the above-mentioned health state estimation methods to ensure enhanced performance and the versatility of the estimation model in different operating conditions [31], [32].

At present, data-driven methods of health state estimation have been widely used in modern energy storage systems and have achieved remarkable results. Such methods are the current research hotspot and future research trends, and a lot of relevant research has been published in recent years. For instance, reference [22] reviews the degradation causes of LIBs by introducing a method based on a classification framework. It also conducts an in-depth analysis of the strengths and weaknesses associated with each method under consideration. In [33], the health state estimation and remaining useful life (RUL) predictions of LIBs are reviewed, the advantages and limitations of BMS applications are discussed, and future development trends and research challenges are analyzed. Reference [34] elaborates on different estimation techniques, challenges, and possible solutions, and also provides recommendations for developing estimation methods for LIBs with the background of the circular economy. Reference [35] discusses the monitoring goals of the health state, summarizes diverse applications from both short-term and long-term perspectives, and thoroughly analyzes the challenges and future trends of health state diagnosis. However, there is still a lack of reviews on energy storage LIBs as the core equipment and advanced neural network models for estimating health states.

Through a comprehensive investigation of a series of ANN-based health state estimation methods presented in recent years, this paper considers the hybrid estimation method based on multi-EIS features and cuckoo search (CS)-Elman neural network (ENN) as a more effective strategy than the methods based on a single physical model or data-driven models. Therefore, this paper conducts a detailed EIS-CS-ENN estimation to obtain the battery health state. To verify the superiority and effectiveness of this model, the values of root mean square error (RMSE), maximum error (MaxE) and mean absolute error (MAE) are used as the key evaluation metrics for the comparison and analysis of different ANN models. By introducing the above evaluation metrics, the characteristics, advantages, and disadvantages of each ANN model are highlighted. The HIs are also adopted to analyze different estimation effects for the same ANN model to verify the significance of the HIs to the results. Finally, this paper examines the current common health state estimation methods, analyzes the research status, constructs an EIS-CS-ENN model for health state estimation, and compares the proposed model with other similar ANN-based methods. Compared to previous related studies, this study, after reviewing and analyzing all types of health status esti-

mation methods, focuses more on an overview of ANN-based health state estimation methods and a specific process for an improved ENN-based health state estimation method.

The rest of the paper is arranged as follows: Section II conducts a detailed analysis and literature survey of different health state estimation methods, including direct measurement, physical model-based, data-driven, and hybrid methods. The establishment of the ANN model, the EIS-CS-ENN-based estimation framework, and the application analysis of the ANN model from other literature are presented in Section III. In Section IV, the effects of different ANN models in estimating health state are compared using several evaluation metrics, and the verification of the superiority of the EIS-CS-ENN-based method is provided. Section V concludes the paper.

II. Analysis of Various Health State Estimation Methods for LIBs

The introduction section has described various approaches, in which the definition of a single battery health state is often divided into capacity-defined and internal resistance-defined methods [35]. In addition, some have put forward other suggestions for health state definition, e.g., defining the health state by monitoring the number of cyclable lithium ions or the solid-phase diffusion time of lithium ions in the positive electrode [36].

As shown in (1), the health state of a system can be defined using either the capacity definition, which calculates the ratio of current capacity to initial capacity, or the internal resistance definition, which calculates the ratio of the difference between the end and current internal resistance to the difference between the end and initial internal resistance.

$$\begin{cases} S_{\mathrm{OH1}} = \dfrac{C}{C_{\mathrm{BOL}}} \\ S_{\mathrm{OH2}} = \dfrac{R_{\mathrm{EOL}} - R}{R_{\mathrm{EOL}} - R_{\mathrm{BOL}}} \end{cases} \tag{1}$$

where S_{OH1} and S_{OH2} indicate the health state of the capacity-defined method and the internal resistance-defined method, respectively; C and C_{BOL} represent the present and initial capacities, respectively; R, R_{EOL}, and R_{BOL} are the present, end of life, and initial internal resistances, respectively. In electric or hybrid electric vehicles, the change in health state primarily results from an increase in battery internal resistance, which impacts the system's energy capability. In addition, new energy storage systems typically experience capacity degradation, which affects the system power capability and defines the change in health state [37], [38].

Generally, when the capacity degrades to 20%–30%, the LIB reaches the end of its life. In addition, some scholars have proposed several methods for defining the health state of battery packs. For example, reference [39] defines the battery pack health state considering grouping and balancing approaches, while [40] defines the health state as the ratio of the current maximum available energy of the battery pack to its original rated energy. Based on the above definitions, various recent papers have proposed and classified a series of battery health state estimation methods from different perspectives, as shown in Fig. 1.

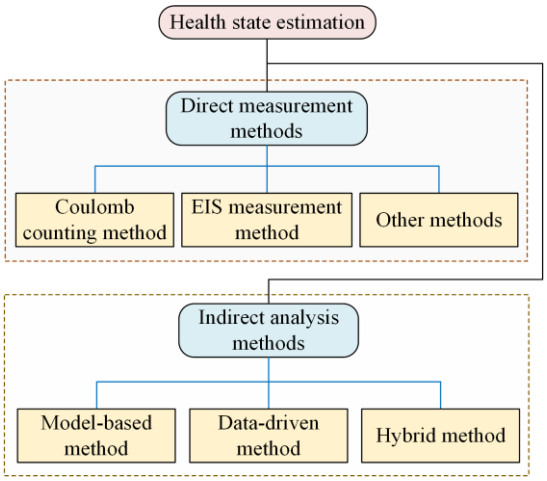

Fig. 1. Classification of health state estimation methods.

As shown in Fig. 1, the battery health state estimation methods divide into two categories: direct and indirect. We will now look at the direct measurement methods and three different indirect analysis methods.

A. Overview of the Direct Measurement Methods

These consist mainly of Coulomb counting and EIS methods. Coulomb counting requires the use of battery charge-discharge equipment to carry out a low-rate discharge experiment on the LIBs, and through the calculation of experimental data, the health state under the complete discharge cycle can be obtained [18], [41], [42]. Specifically, Coulomb counting requires experimental instruments to obtain the current, time, and initial and end states of charge (SOCs) of a complete discharge cycle in a low-rate constant current (CC) discharge condition.

The difference between current integral and SOC is obtained by integration, and their ratio is the health state of the LIB at this time. However, in the battery degradation process, since this method relies on the SOC difference and current integration, the error is relatively large, and the error accumulates gradually [43]. The EIS method directly uses a wide spectrum to determine the health state of LIBs. This method is based on frequency domain analysis, and involves measuring the response of LIBs to sine-wave excitation across a wide range of frequencies. The impedance is then calculated from the ratio of the excitation voltage to the response current,

which serves as a factor for characterizing the health state. A typical Nyquist plot obtained using the EIS method is shown in Fig. 2.

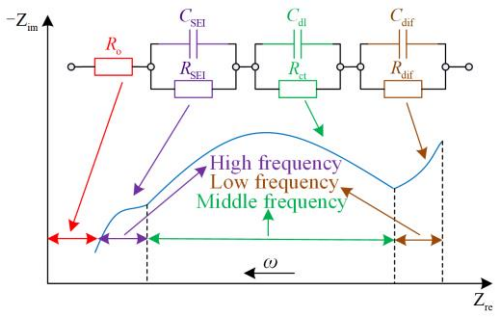

Fig. 2. Typical Nyquist plot obtained using the EIS method.

As shown in Fig. 2, the Nyquist plot consists of three parts: low, middle, and high frequencies. Wherein, R_o denotes ohmic resistance, C_{dl} denotes double layer capacitance, and R_{ct} denotes charge transfer resistance. Additionally, C_{SEI} and R_{SEI} represent solid electrolyte interface (SEI) film capacitance and SEI film resistance, while C_{dif} and R_{dif} signify diffusion capacitance and diffusion resistance. The low-frequency range is associated with the diffusion kinetics that occur within the electrodes, the middle-frequency range is linked to the charge transfer reaction and the double layer capacitance effect, while the high-frequency range is associated with the SEI film and the solid-phase contact resistance [35]. In the EIS test, some parameters show obvious trends with battery degradation, such as R_{SEI} and R_{ct}. From the findings in [44], these parameters exhibit promising potential in accurately estimating the health state.

While the EIS method offers high-precision measurements and can provide detailed information on the electrochemical reaction process by decomposing the impedance, it necessitates specialized measurement technology, complex test equipment, and a long duration, which make it difficult to apply in engineering conditions [45], [46]. Other direct measurement methods include the internal resistance measurement, cycle counting, and destructive test. The internal resistance measurement method involves measuring the battery's internal resistance online to obtain its health state [47]. Because of the small internal resistance, this method requires an accurate measurement circuit to be acceptable. The cycle counting method determines the health state by obtaining the maximum number of full discharge times for the LIB [29]. This method only needs to number and count the full charging-discharging cycles, and is usually used in laptops or small electronic devices. However, since this method strongly relies on the rated number of discharges, the estimation accuracy is low, and thus is not suitable for energy storage systems. The destructive test method studies the degradation mechanism of LIBs by disassembling them to obtain the health state from a microscopic point of view. However, this method will cause irreversible damage to LIBs when being studied using Raman spectroscopy [48], X-ray diffraction [49], and X-ray photoelectron spectroscopy [50]. Therefore, this method is not applicable for real-time engineering requirements.

To more clearly demonstrate the differences among the above-mentioned methods, the advantages, disadvantages, and research status of various direct measurement methods are analyzed, as shown in Fig. 3. In addition, in the above-mentioned direct measurement methods, the extraction features and research directions are different from each other, as summarized in Table I. As seen, it is evident that different direct measurement methods have their own extraction features and research directions, and thus, in the corresponding field, each method is essential and has the potential for improvement and optimization.

TABLE I
THE EXTRACTION FEATURES AND RESEARCH DIRECTIONS OF DIRECT MEASUREMENT METHODS

Direct measurement methods	Extraction features	Research directions
Coulomb counting method	The current and time of a complete discharge cycle under the low-rate CC condition	This method is recommended to improve it with filtering methods
EIS method	The excitation voltage and response current in EIS test	This method is recommended to improve it with dynamic EIS or fractional order theory
Internal resistance measurement method	Step changes of current and voltage in charge-discharge curves	This method is recommended to improve it with data-driven methods
Cycle counting method	The number of full charging and discharging cycles	This method is recommended to improve it with data-driven methods
Destructive test method	Changes of battery internal micro-structure during degradation	This method is recommended to explore more precise equipment and approaches

B. Overview of the Physical Model-based Methods

Physical model-based health state estimation methods can be described from different perspectives. This kind of method cannot be separated from the internal reactions and external characteristics of LIBs. The block diagram of physical model-based health state estimation methods is shown in Fig. 4. The process here of health state estimation is divided into three parts: model selection, parameter identification, and health state estimation. In this review, physical model-based health state estimation approaches are divided into two categories: ECM-based and EM-based methods.

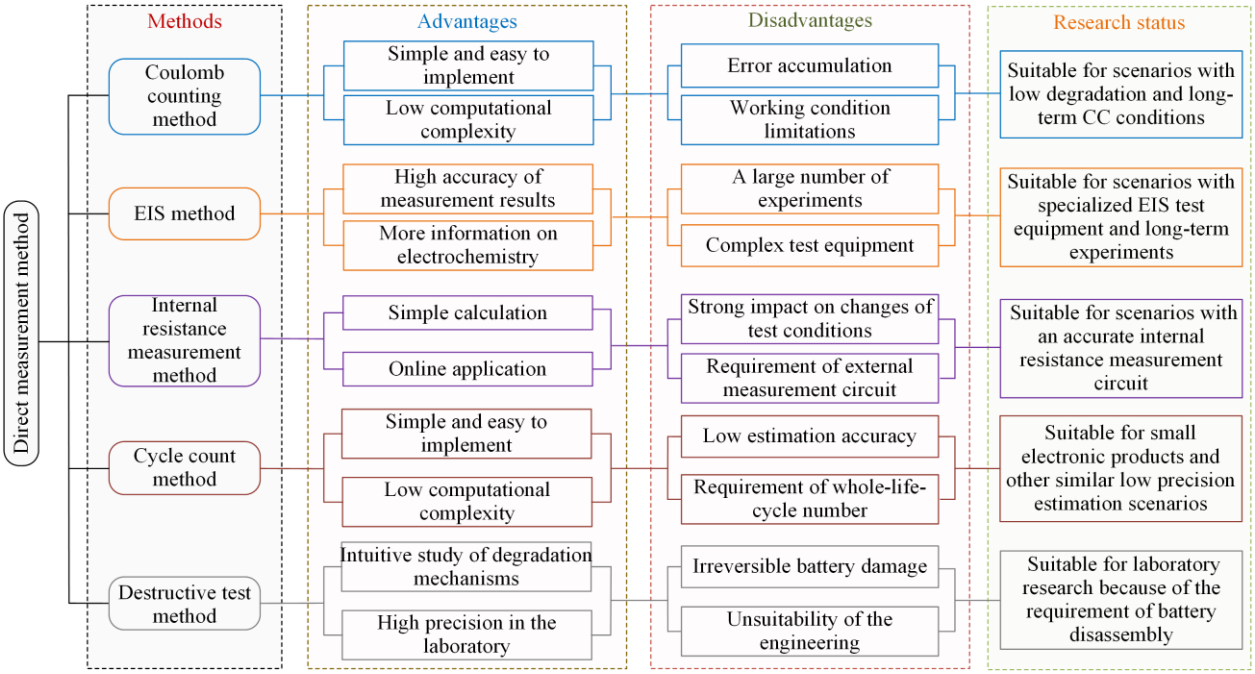

Fig. 3. The advantages, disadvantages and research status of various direct measurement methods.

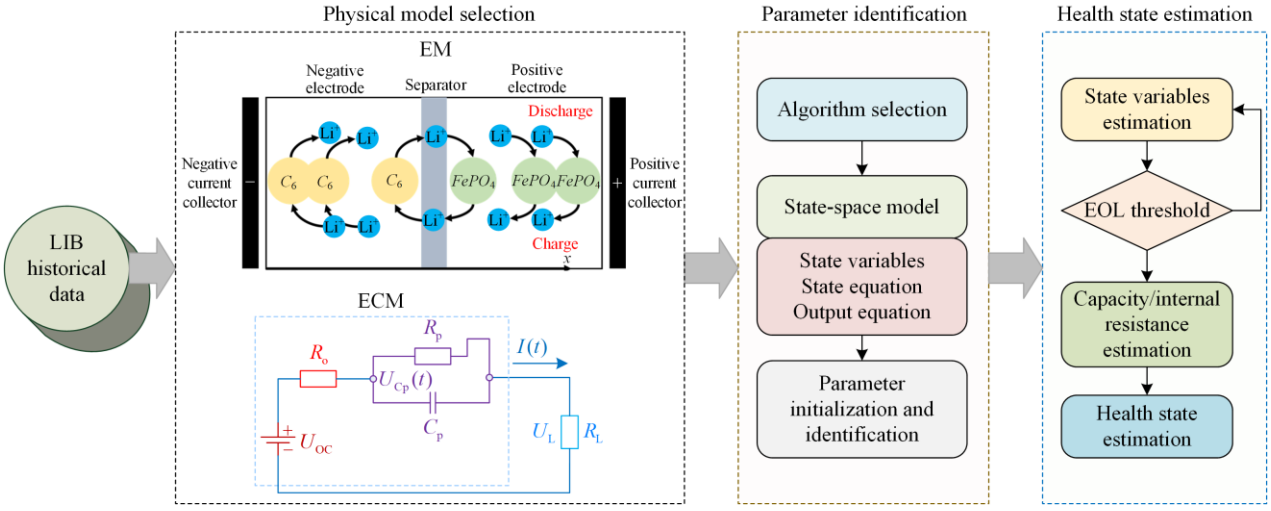

Fig. 4. The block diagram of physical model-based health state estimation methods.

1) ECM-based Methods

ECM simulates the dynamic voltage characteristics of LIBs based on power supply, inductance, capacitance, resistance, and other circuit components, and is established based on Kirchhoff's circuit law. Each parameter incorporated within the model possesses distinct and well-defined physical interpretations, coupled with straightforward mathematical expressions, rendering the model comprehensible and interpretable [31]. Common ECM models include the Rint model, a variant order of the Thevenin and resistor-capacitor (RC) models, partnership for a new generation of vehicles (PNGV) models, and general nonlinear (GNL) models [25], [51], [52].

In addition, some have investigated a series of improved composite models based on the above ECMs. For instance, reference [53] develops an improved second-order RC model by adding a high capacitance and a current control current source. Also, with a Thevenin ECM and the open-circuit voltage hysteresis characteristics, reference [54] establishes a variable-parameter equivalent hysteresis model. In [55], an improved first-order RC model is developed considering the current direction and hysteresis effects based on the research of [56]. From different perspectives, references [57] and [58] propose fractional-order ECMs, while the performance of the integer-order and fractional-order models in estimating battery state are analyzed in different operating conditions [59]. In [60], a comparison of twelve ECMs is conducted based on their complexity, accuracy, and robustness in varying operating conditions and temperatures. Their findings reveal that the first-order RC model with the hysteresis effect

is the most appropriate for describing lithium iron phosphate batteries.

The ECM-based health state estimation methods need to design an experimental scheme to identify parameters and indirectly estimate the health state through the parameters and state variables. ECM parameter identification approaches incorporate two categories: offline curve fitting and online least squares (LS) methods [22]. The curve fitting comparison method, based on the hybrid pulse power characterization test, calculates the direct-current internal resistance by analyzing the voltage change caused by the pulse current. Once the pulse charge-discharge is complete, a time-domain circuit equation is formulated to obtain the polarization resistance and capacitance through comparison with the fitting curve. Because of its offline property, the calculation is simple, but the time-varying parameters of the LIBs are not accurately characterized, resulting in large errors.

The parameter identification of ECM based on the LS method is carried out by establishing the circuit equation in the complex frequency domain using the traditional model or its improved forms. To acquire the optimal results, these methods update the model parameters continuously by minimizing the output error between the model and reality [33]. Among the various improved forms of the LS method, the recursive least squares (RLS) method is the most common online identification method. Reference [61] applies the RLS method to the parameter identification of an improved ECM, and the verification results show that the RLS method can obtain the ECM parameters online with good results.

In addition, the RLS method has also been modified and optimized. For example, reference [62] proposes a novel RLS method, which incorporates optimum multiple adaptive forgetting factors (MAFF), to identify time-varying electrical parameters of the ECM. This method is used for SOC and health state estimation of LIBs. The performance of the optimum MAFF-RLS method is compared to that of the RLS method with multiple fixed forgetting factors, and the results show that the optimum MAFF-RLS has better performance on many evaluation indicators. Reference [63] improves a parameter identification method based on RLS with a sliding window difference forgetting factor to identify ECM parameters. The results demonstrate that this novel method can effectively use new data for different conditions, and while improving the parameter convergence speed, the robustness and accuracy of the parameter identification results are also guaranteed.

After successfully identifying the ECM parameters, they are used to estimate the health state along with filtering algorithms. The ECM and filtering algorithms are combined to estimate either the internal resistance or the capacity. These can reflect the changes in health state. To achieve this, a state space model is formed by constructing state-space equations. Specifically, the expression of internal resistance or capacity is adopted as the state equation, the voltage expression is adopted as the observation equation, and a filtering algorithm is used to calculate the health state iteratively.

The filtering algorithm exploits the internal recursive relationship of the system states to obtain data and time changes. The most common and representative filtering algorithm is the Kalman filter and its variants, but because of the strong nonlinearity and high computation characteristics of LIBs, a series of improved filtering algorithms have been proposed. Double extended Kalman (DEKF) [15], [64], adaptive extended Kalman (AEKF) [65], unscented Kalman (UKF) [53] and particle (PF) [66] are the most common filters. The above algorithms need to go through several steps of initialization, prediction and updating to obtain accurate results. Reference [67] presents a method for jointly estimating SOC and health state, called the bias compensation recursive least square-multiple weighted DEKF method, which is based on a second-order ECM. Since the method introduces bias compensation to improve RLS, it can reduce the impact of colored noise on the system. In [68], the battery SOC and health state are simultaneously estimated using multi-innovation UKF (MIUKF) and UKF, verifying the effectiveness of the cooperative estimation method. Reference [69] develops a health state estimation method based on the second-order ECM and genetic resample particle filtering. The availability of this approach is verified under the Beijing bus dynamic street test working condition.

2) EM-based Methods

Intercalation and deintercalation of lithium ions occur continuously during the use of LIBs, resulting in the continuous generation and rupture of SEI, which leads to changes in the internal mechanism. Based on this principle, an EM known as the pseudo-two-dimensional (P2D) model is proposed, which uses a series of nonlinear coupled partial differential equations [70]. Within this model, the battery anode and cathode are treated as porous electrodes made up of numerous spherical particles, and the interstitial spaces between the particles are completely filled with electrolytes.

The P2D model simulates the whole battery structure, including all the basic components of LIBs, and this enables EM to describe the electrochemical kinetics. The P2D model also fully takes into account the processes of solid- and liquid-phase diffusion and migration in the battery reaction. It is thus usually regarded as the benchmark mechanism model of EM, and lays the foundation for EM development. The principles and challenges of EM are shown in Fig. 5.

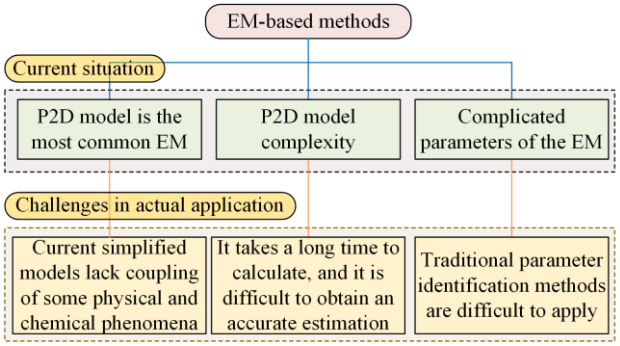

Fig. 5. Principles and challenges of the EM-based methods.

However, the P2D model contains a lot of nonlinear equations, which lead to its high difficulty and low computational efficiency [71]. In addition, when identifying numerous parameters in the P2D model, it is inevitable to encounter overfitting or local minimization problems. These problems hinder the application of the P2D model in practical engineering, so it is necessary to simplify it for practice [72]. Significant research has been devoted to the simplification of the P2D model in recent years, and simplified models in different multi-scale technologies have been proposed [73].

The first type of simplification for EM involves reducing the order and complexity of the equations and expressions. The second type is to ignore the process with little influence on external characteristics based on the P2D model, so as to simplify the model structure or parameters. For the first simplification, reference [74] proposes an EM with a simplified side reaction transfer function, whereas [75], [76] use the discrete-time realization method to decrease the order of some differential equations that describe the porous electrode theory in the P2D model. In [77], the polynomial approximation principle is proposed to decrease the order of the P2D model.

For the second simplification, the single particle (SP) model and its related extended single particle (ESP) model are proposed [78]. The SP model is the most mature and representative simplified model in EMs. It ignores the concentrative distribution of electrolyte concentration gradient, liquid-phase diffusion overpotential, and solid concentration in the direction of electrode thickness, and uses a single particle to depict the concentration distribution of lithium ions within the electrodes. Compared with the P2D model, the SP model has the strengths of simple structure and fewer calculations, but the simulation effect is poorer at a high rate.

The SP model is of great significance in the field of health state estimation and has been used in some situations [79]. For example, reference [80] developed a health state estimation method for BMS by combining an improved capacity degradation model and an SP model. The ESP model considers the internal structure, reaction process, and environmental factors on the basis of the SP model to optimize the model accuracy and the versatility of the working conditions. Reference [81] presents an improved SP model considering the overpotential and spatial variation of open-circuit potential to estimate battery states, while [82] introduces the electrolytic phase potential difference into the SP model and considers the influence of unmodeled dynamics. The results indicate that this method offers a certain improvement in calculation efficiency and estimation results. Based on the SP model, reference [83] develops and illustrates a single particle model with electrolyte (SPME) considering the influencing effect of the electrolyte on the output voltage. By introducing the law of matter conservation in liquid electrolytes and the law of charge conservation, the model accuracy is improved. In [84], an ESP model considering concentration overpotential is established to estimate the health state of LIBs.

When using EM to estimate the health state, it is often combined with filtering algorithms. The principle of the EM-based filtering algorithms is the same as that of the ECM-based filtering algorithms. In the EM-based filtering algorithms, the capacity and internal resistance are usually selected as the HIs and state variables. References [85], [86], and [87] put forward approaches to estimate the internal resistance and capacity with proportion-integration (PI) multi-time-scale observers, and EKF-PF methods, respectively.

Electrochemical parameters such as the number of lithium ions that can be recycled in the electrodes and the maximum concentration of solid-phase lithium ions in the cathode and anode can also serve as HIs. The electrochemical parameters change monotonously with the battery degradation, but the disadvantage of selecting those parameters as HIs is that the results are difficult to fully verify. For example, reference [88] creates an adaptive partial differential equation observer to determine the internal resistance and the number of cyclable lithium ions, and these are used as HIs to evaluate the health state. Reference [89] uses the linear decreasing weight-particle swarm optimization technique to identify electrochemical parameters and extracts the maximum solid-phase lithium-ion concentration of cathode and anode as the HIs. Some have combined EM with capacity degradation mechanisms to reflect the specific causes of degradation quantitatively, but this field is still in the exploratory stage.

The above-mentioned review describes the recent advanced technologies and specific implementation approaches of ECM-based and EM-based estimation methods. The current advantages, disadvantages and research status of ECM-based and EM-based health state estimation methods are summarized in Fig. 6.

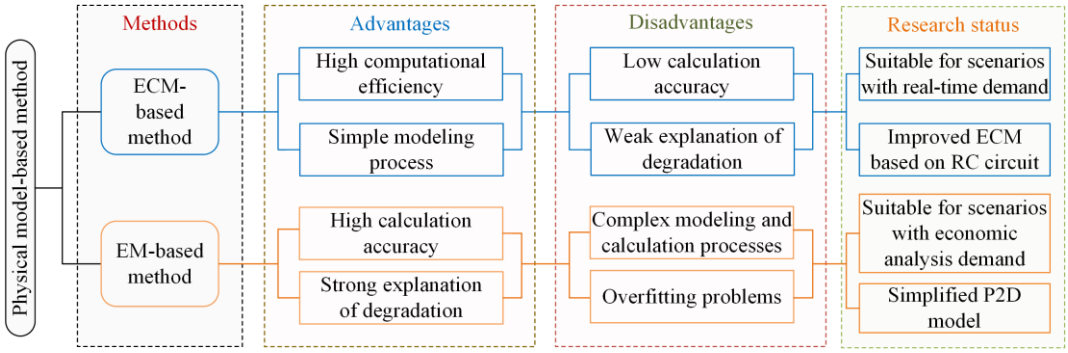

Fig. 6. The advantages, disadvantages and research status of physical model-based methods.

It is evident that the ECM-based method is more suitable for the real-time analysis environment, while the EM-based method is more suitable for the environment of electrochemical material economic analysis.

C. Overview of the Data-driven Methods

Because of the high complexity and nonlinearity of LIBs, it is a challenging endeavor to establish a physical model that applies to a variety of operating conditions. The data-driven method does not consider the internal reaction of LIBs and only depends on the analysis and extraction of massive amounts of collected data. It is noteworthy that while data-driven methods demonstrate efficacy in handling nonlinear problems, they are susceptible to the influence of training data sets and methodologies, warranting careful consideration and scrutiny [90]. Fortunately, the emergence of big data platforms has introduced a solution to this problem. Data-driven health state estimation methods include different approaches [30], [72], [91]. This review classifies the data-driven methods into two categories: ML-based and DA-based. ML-based methods usually include ANN, SVM, RVM, and FL, whereas the ICA and DVA methods are two of the most common DA-based methods.

1) ML-based Data-driven Methods

ML is a method of analyzing massive amounts of data by automatically building models. The main idea is to analyze the model through data learning and recognition, making decisions as autonomously as possible. The generic workflow of the ML model for health state estimation is illustrated in Fig. 7.

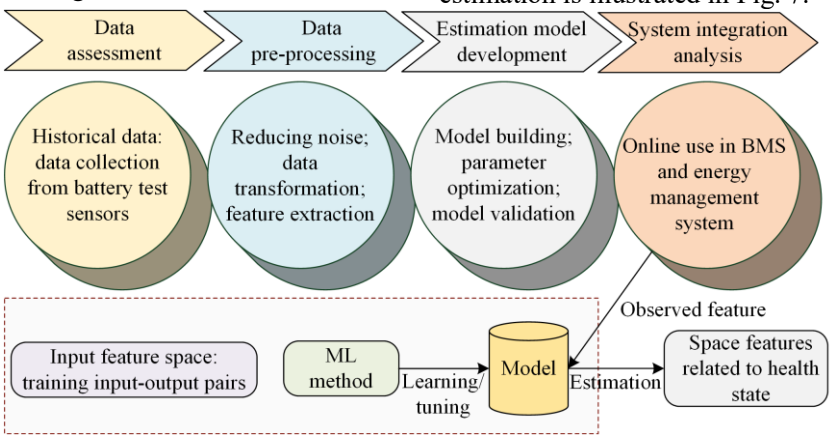

Fig. 7. Generic workflow of the ML model for estimating health state.

Here using ML is divided into data accessing, data pre-processing, estimation model development, and integrating analytics with systems. In data assessment, the measurable parameters are recorded, including current, voltage, and temperature, during the operation of LIBs in energy storage systems. Because the measurable data are not all related to health state and battery degradation, data pre-processing is introduced. In this step, the features closely related to the health states of LIBs, also known as HIs, are extracted. After the features are extracted and organized, the estimation model development is carried out. In this step, features and health states are taken as inputs and outputs of the ML model to train the model, describing the relationship between features and health states. To integrate analytics with systems, the trained ML model is used in the BMS for estimating the health state to meet the engineering needs. The extraction of HIs is essential to the estimation, and how to select these HIs significantly impacts the effectiveness and accuracy of the ML-based method.

As an improved ML method, ANN simulates brain behavior and arranges artificial neurons in input, hidden, and output layers. Although the parameters of ANN cannot directly reflect the physical or chemical structure, it has a strong nonlinear mapping ability and can be

used to describe LIBs with complex nonlinear characteristics [23], [92], [93]. Neurons within adjacent layers of ANN are interconnected, while those within the same layer are independent of each other. Within the framework, each neuron is characterized by a weighted linear amalgamation, wherein the weighting method is contingent upon the mathematical model's input directed to the neuron.

ANN-based health state estimation methods are often used because of their high accuracy and autonomy [91]. ANN has a wide range of network choices. The feedforward neural network (FFNN) and recurrent neural network (RNN) are the two most common types and are both based on time series. Reference [94] constructs the terminal voltage in the constant current charging process as the input of the FFNN model to obtain the predicted remaining useful life and the estimated health state. FFNN uses a backpropagation neural network (BPNN) to train the estimation model. Specifically, reference [95] inputs the identification results of the Thevenin ECM into a three-layer BPNN model in the training process for the health state estimation, whereas [96] extracts two HIs with a strong correlation from the incremental capacity (IC) curve as the input of the FFNN model to jointly estimate the battery health state and RUL.

As a special kind of RNN, long short-term memory (LSTM) is also adopted for estimation. After expounding on the advantages and disadvantages of traditional RNN and LSTM, reference [97] estimates the health state by combining their structures and realizing adaptive time series prediction. Given that LSTM has basic learning information, reference [98] creates an active state tracking-LSTM neural network for filtering more relevant information to realize the LSTM estimation model shared by multiple LIBs.

SVM is a non-parametric model on the basis of the kernel function, and belongs to the supervised ML method [99]. The core idea of SVM is to find a subset of critical support vectors that can describe the system from massive data and to use regression methods to transform low-dimensional nonlinear models into high-dimensional linear models [100]. The advantage of SVM is its flexibility, and when the amount of data is large enough, any system model can be established, while the processing capability is very powerful when the amount of data is small [27], [101]. Therefore, various battery states, including the health state, can be accurately estimated using SVM [19]. However, for SVM, optimizing the kernel function and hyperparameters for nonlinear modeling can be challenging [102]. Reference [103] develops an optimized SVM-based estimation method considering the changes of temperature, SOC, and charge-discharge rate. In this method, two-thirds of the collected data are adopted for training, and the remaining data are used for testing.

In addition to the basic SVM, some improved SVM models have been proposed. Reference [27] develops a two-layer structure SVM with radial basis function for efficient estimation of health state. For this method, the selection of appropriate cost functions is the key to obtaining accurate results. In [104], an optimized SVM is created to capture capacity degradation for RUL prediction and health state estimation. The improved core of this method is to use the particle swarm method to optimize the kernel parameters of the SVM. The improved SVM can estimate the change of health state with battery degradation well so that the results are hardly disturbed by local regeneration and fluctuation.

Since the SVM method cannot output credible intervals, RVM is proposed as its variant for estimation and prediction, but it is less used in practical applications. RVM shares the same main concept as SVM, but takes a probability-based approach. Unlike SVM, RVM can construct arbitrary kernel functions without limitations [105]. In addition, SVM requires initial manual parameters, while RVM does not. The sparse model benefits arbitrary kernel functions with high sparsity, making numerous weights zero, which can speed up the operating efficiency. The determination of kernel function weights in RVM is critical. The strengths of RVM include high accuracy, strong learning ability, good sparsity, and a simple training process, whereas its weaknesses include massive training data samples and a long training time.

In recent years, there have been some applications based on SVM. Reference [105] proposes an intelligent health prognosis that takes the optimal embedding dimension as the RVM input, and among them, the optimal embedding dimension is obtained using the time series reconstruction method based on mean entropy. Reference [106] adopts RVM to obtain relevance vectors that can denote capacity degradation, and the degradation of the health state can be estimated through relevance vectors. In [107], a method is developed for RUL prediction and health state monitoring with two discharging voltage difference features as inputs to the RVM.

FL is a bionic reasoning method that simulates the human brain. It uses the FL theory to deal with the problem of solving complex and nonlinear systems with fuzzy phenomena. The measurement data of nonlinear systems with fuzzy phenomena is divided into clear sets and fuzzy sets, where the fuzzy sets contain uncertain data. The members of fuzzy sets belong to the membership function (MF), and the FL can distinguish fuzzy sets and deal with fuzzy relations through MF. The selection of MF is the key to estimating an accurate health state [23], [108]. In [109], a fuzzy information granulation method is proposed for the estimation of the health state range, while [110] fits the curve of capacity degradation through an optimized FL controller and effectively estimates the health index in different working conditions to indirectly express the current

health state of LIBs.

2) DA-based Data-driven Methods

The central concept behind DA-based methods is to identify features linked to capacity degradation from differentiated curves in electrical, thermal, or mechanical parameters during battery operation [111]. Since these curves can only be obtained when the LIB is under low-rate constant current charging or discharging conditions, the application of such methods in complex conditions is limited. Recently, DA methods such as ICA and DVA have attracted great attention in the study of degradation mechanisms and capacity loss estimation methods, and have made some progress in the field of health state estimation [112]. In ICA and DVA methods, there is no need for irreversible damage to LIBs, and they have been widely used in degradation research [113].

Specifically, ICA and DVA methods estimate the health state by extracting features, so they can intuitively reflect the battery health state without building physical or mathematical models [114]. Compared with ML-based methods, DA-based methods require fewer data types and are more intuitive, but the differentiated curves of such methods have noise that cannot be eliminated, and the process of extracting HIs is challenging. In addition, DA-based methods are highly dependent on low-rate constant current conditions, so they are not very versatile in practical energy storage systems. The open-circuit voltage curves exhibit a flat and coincident behavior under constant current conditions, making it challenging to differentiate the variations among different curves directly. However, the ICA and DVA methods can convert the flat voltage stage into features of corresponding differentiated curves. Specifically, the ICA and DVA methods can convert the flat voltage stage into peaks in the IC curve and valleys in the differential voltage (DV) curve, respectively, each of which characterizes a specific battery electrochemical process [115].

Observing changes in IC and DV curves can establish the correlation between external and internal characteristics of LIBs. High-rate conditions hinder complete intercalation and deintercalation of lithium ions, resulting in altered battery performance. In addition, high-rate conditions induce an upsurge in polarization current, elevating internal resistance and causing the battery to reach the charge-discharge cut-off voltage in advance, leading to decreased battery capacity. Therefore, to study degradation, the ICA and DVA methods usually use low-rate currents for experiments. It is worth noting that when charging from different SOC, the peak position on the DV curve will change greatly because of the change in the charging capacity, but the peak position of the IC curve does not have this problem. This results in the ICA method being more suitable for online health state estimation than the DVA method [116].

Since the ICA and DVA methods only need to monitor voltage and battery reserve capacity and do not need to establish physical and mathematical models, some have proposed a series of related estimation methods [117]. For example, reference [118] develops an online technique for LIBs based on incremental voltage difference, and introduces a new feature vector to solve the problem that the health state cannot be accurately estimated when the charging data is lacking. The feature vector consists of the difference between the voltage and the mean temperature, and reference [119] creates a method for BMS that uses the peak interval of the DV curve to estimate the health state for lithium iron phosphate cells, and validates the results in a data set of 18 cells.

The above-mentioned review investigates the recent advanced technologies and corresponding estimation effects of the ML- and DA-based methods. The current advantages, disadvantages, and research status of ML-based and DA-based health state estimation methods, are summarized in Fig. 8. On the one hand, with the iteration of hardware and data analysis software, the ML-based method is widely used for whole-life-cycle estimation. On the other hand, the DA-based method is more commonly used for health state analysis of a certain charging and discharging cycle.

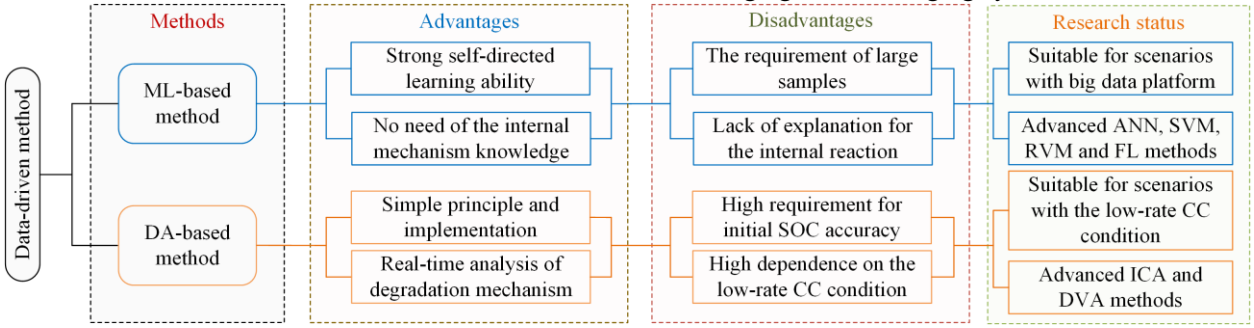

Fig. 8. The advantages, disadvantages and research status of data-driven methods.

D. Overview of the Hybrid Methods

Physical model-based methods are difficult to balance in computation and estimation accuracy, whereas data-driven methods strongly rely on data quality and the selection of HIs. Hybrid methods can complement the above two methods, and as a result, hybrid state

estimation methods have gained considerable attention in related research fields in recent years. As the name suggests, a hybrid method refers to an amalgamation of two or more methods, and can include the same type or a combination of different types of methods. Compared with the single method, the hybrid method has higher accuracy and versatility. In this review, hybrid methods are divided into five types considering the different combinations of: direct measurement and physical model-based; direct measurement and data-driven; data-driven and physical model-based; different physical model-based; and different data-driven methods.

For the combination of direct measurement and physical model-based methods, reference [120] presents a method on the basis of EIS and the double polarization model. Specifically, after extracting the double polarization model from EIS, the forgetting factor recursive least squares (FFRLS) method is used for parameter identification and the correlation between parameter changes and the degree of degradation is studied. Finally, the health state is estimated by the correlation between SEI film resistance and residual capacity.

For the combination of direct measurement and data-driven methods, reference [121] measures the difference in impedance before and after battery degradation, and concludes that the battery health state is related to the impedance. Specifically, an improved FL model is established, and the EIS measurement data of two different degradation conditions are regarded as the model input for the health state estimation.

For the combination of data-driven and physical model-based methods, references [122] and [123] concur that the health state of LIBs can be estimated by combining ECM with a data-driven method. In [122], a co-estimation method is proposed for the health state and power state estimation of a series of LIB packs based on model prediction and FL, whereas in [123], a health state estimation idea is proposed and verified based on Thevenin ECM and a multivariate autoregressive method. This is used for real-time capacity estimation and prediction when the amount of measured data is insufficient. In addition, reference [124] extracts multiple physical features from mechanical and electrochemical models as the input to Gaussian process regression, and the results demonstrate that the estimation error of this approach is low for all test datasets.

For the combination of different physical model-based methods, reference [125] combines the electrochemical mechanism and ECM, considering the constant-phase-element (CPE), to construct a hybrid model to estimate the battery states. In this method, an ECM that can characterize the electrochemical reaction inside LIBs is developed based on the Nyquist impedance diagram for battery state estimation. This hybrid EM-ECM approach considers both external and internal electrochemical characteristics of LIBs. However, there are few application and engineering examples because of the difficult calculations and theories.

For the combination of different data-driven methods, building upon the multi-feature fusion models using a stacking mechanism, reference [126] proposes a method to estimate the health state of power batteries, in which SVR and LSTM are integrated to estimate battery health state by combining various feature parameters. The outcomes demonstrate that this novel approach enhances multi-feature fusion performance and improves estimation accuracy. Reference [127] establishes a hybrid model based on an autoregressive moving average and ENN for long-term health state estimation. Among them, the constant charging time is selected as a HI to be input into the ENN.

The advantages, disadvantages and research status of the five hybrid methods are summarized in Fig. 9. Compared to a single estimation method, the accuracy and implementation difficulty of the hybrid methods increase. The detailed evaluation results of the hybrid methods for health state estimation are shown in Table II. It can be observed from Table II that the different hybrid methods have their respective advantages in terms of computational complexity and accuracy of experimental results.

TABLE II
THE DETAILED EVALUATION RESULTS OF HYBRID METHODS FOR HEALTH STATE ESTIMATION

Hybrid methods	Calculation data	Evaluation index	Accuracy
Direct measurement + physical model-based method [120]	Double polarization model + FFRLS	Error	<3%
Direct measurement + data-driven method [123]	Matrix operation + EIS + FL	MAE	0.5183%
Physical model-based + data-driven method [123]	Matrix operation + DEKF + autoregressive model		
Different physical model-based methods [125]	Reduced-order model of P2D + CPE		
Different data-driven methods [126]	Matrix operation + SVM + LSTM	RMSE/ MAPE	Reduced by at least 0.11%–0.12%

The advantages, disadvantages, and improvement directions of the diverse methods are described in Fig.10.

The direct measurement method is more suitable for the experimental environment, while the physical model-based and data-driven methods are more suitable for the engineering environment. The hybrid method is the most widely used in practice. The above approaches are mostly used to estimate the cell health state during the operation of the battery pack for electronic devices. Therefore, more research and breakthroughs are needed to accurately estimate the health state of inconsistent battery packs.

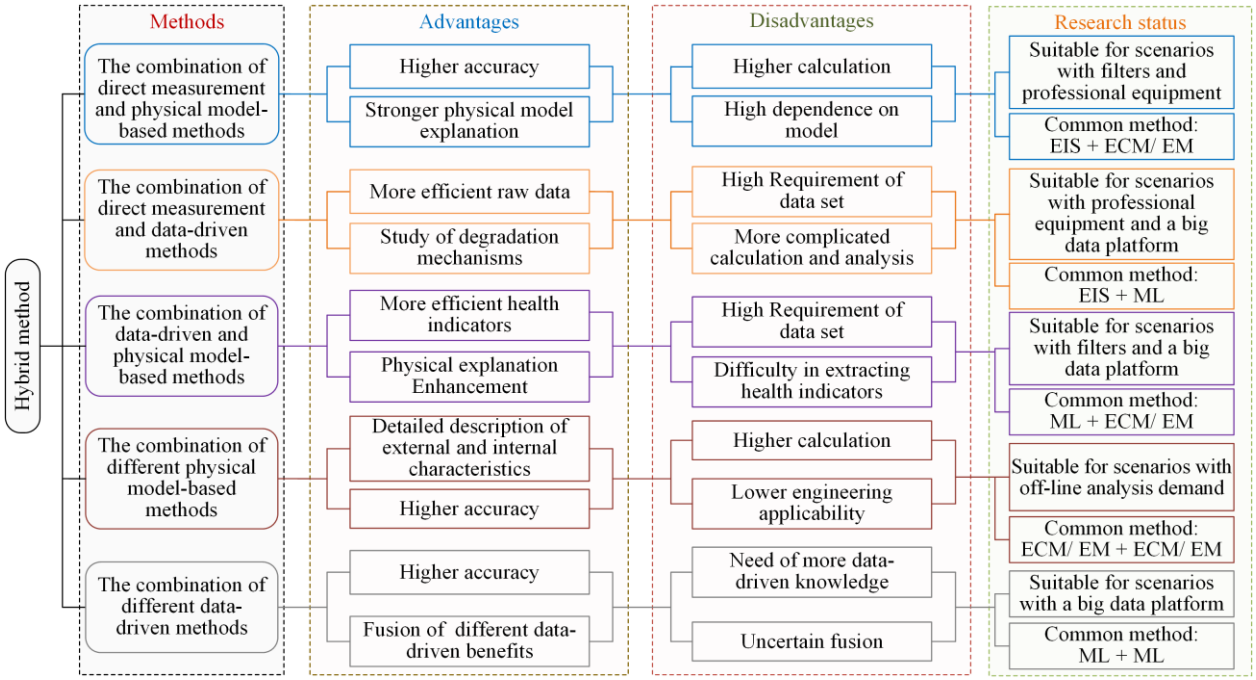

Fig. 9. The advantages, disadvantages and research status of five hybrid methods.

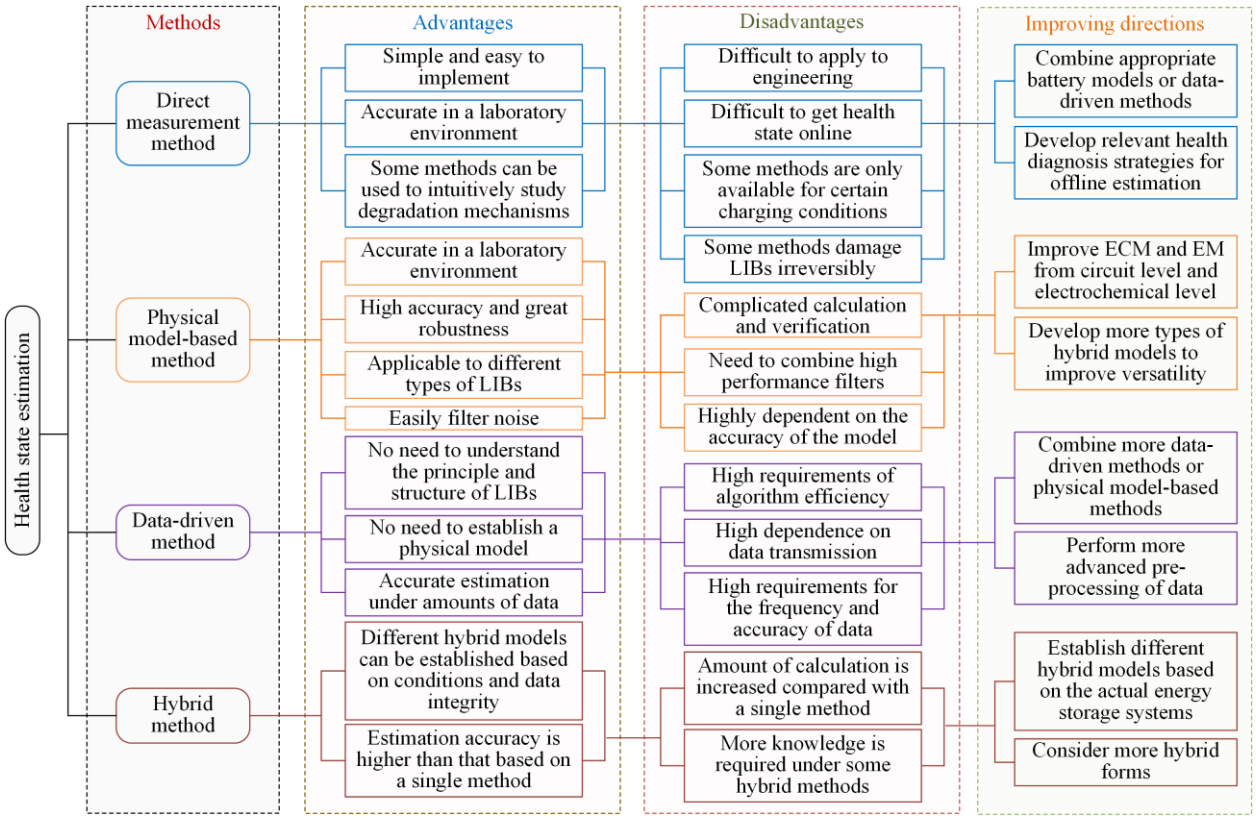

Fig. 10. Comparison of four health state estimation methods.

III. Improved Elman Neural Network for Health State Estimation

In this section, the modeling process of different ANNs is described, the specific structure and estimation process of the improved ENN method are analyzed, and the strengths and weaknesses of different ANNs in estimation are compared.

A. Mathematical Modeling of Artificial Neural Networks

ANN is a practical and straightforward model frequently employed for solving nonlinear problems.

However, because of the intricate nature of the internal electrochemical reaction, the LIB is a highly complex nonlinear system. Generally, the structure of an ANN includes the input layer, hidden layer, and output layer, with each layer having several neurons. The input layer transmits the received information to the hidden layer, and after the weighted linear calculation of each neuron in the hidden layer, the information propagates to the next hidden layer or output layer. In the hidden layer, each neuron provides input and output functions, which are expressed through the mathematical model of the activation function [128].

The weight of a neuron is essential to its input and output. It represents the strength of the connection between neurons, and is adjusted and determined by the learning process of the ANN. There are many ANN methods developed to estimate battery states in energy storage systems. Researchers have categorized ANN methods into traditional ANN and deep learning (DL). These have been successfully and widely employed to estimate the health state of LIBs [129]. The differences and relationships between different ANN methods are shown in Fig. 11.

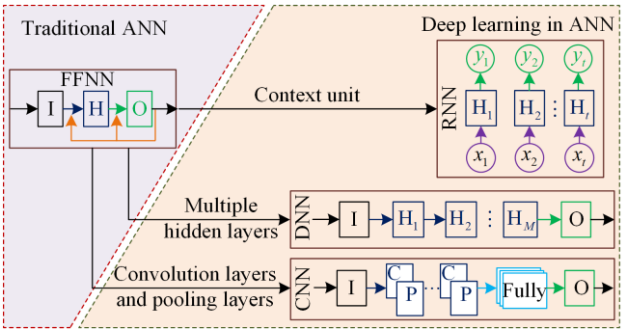

Fig. 11. Differences and relationships between different ANN methods.

The traditional ANN generally refers to FFNN, and the model contains only one hidden layer (H), while the input (I) data only propagates in one direction. Based on FFNN, selecting appropriate HIs as the input of the model is the most critical task. The structure of the FFNN is shown in Fig. 12(a).

The sample entropy of discharge voltage [130], the peak value of the IC curve [96], [131] the change of voltage [132], the model parameters [133], and the change of SOC [134] have been used as HIs in different environments and to meet different requirements. Plotting the smooth IC curve is very important when obtaining the peak value of the IC curve.

Multiple hidden layers are described in the DL model [135], and DL generally includes RNN [136], deep neural network (DNN) [137], and convolutional neural network (CNN) [138]. The 2D input CNN includes one or more convolutional and pooling layers, fully connected layers, and an output layer. DNN is a direct extension of FFNN. The DNN model contains multiple hidden layers, and information is transmitted by one or more hidden layers activated by the activation function. RNN has had significant achievements in estimating the health state of LIBs in energy storage systems. RNN extends a feedback connection based on FFNN to store historical information, and the structure of the RNN is shown in Fig. 12 (b). This improvement enables RNNs to handle large amounts of sequential data in dynamic systems.

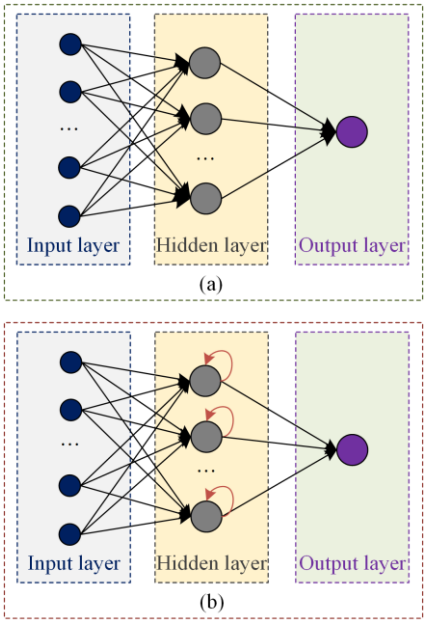

Fig. 12. Differences and relationships between different ANN methods. (a) FFNN. (b) RNN.

Specifically, in battery systems, information can be captured and updated from degradation data for state estimation and prediction during degradation. As the most basic RNN, the structure of an ENN is shown in Fig. 13, where k denotes the current time point, $x_{i,p}^{\mathrm{In}}$ denotes the pth input of the ith sample time point, w_{pq}^{H} denotes the weight connecting the input and hidden neurons, v_p denotes the weight connecting the context unit and the hidden neuron, and b denotes the bias vector. At each time point, the output is determined by the input with the previous value stored in context units.

The characteristic of a normal RNN in estimating health state is that it has to understand and rely on the previous behavior of the LIBs. The advantage of a normal RNN over FFNN is its ability to construct a more accurate model in a time-dependent environment. However, the presence of long-term dependencies in traditional RNNs can give rise to the issues of gradient disappearance or explosion during the backpropagation through time, and therefore, as a special RNN, LSTM is proposed for health state estimation. In LSTM, the gating mechanism is used to solve the propagation of gradient problems [139]. LSTM has a different architecture from ENN, and the LSTM layer uses three gates to connect neurons, as shown in Fig. 14.

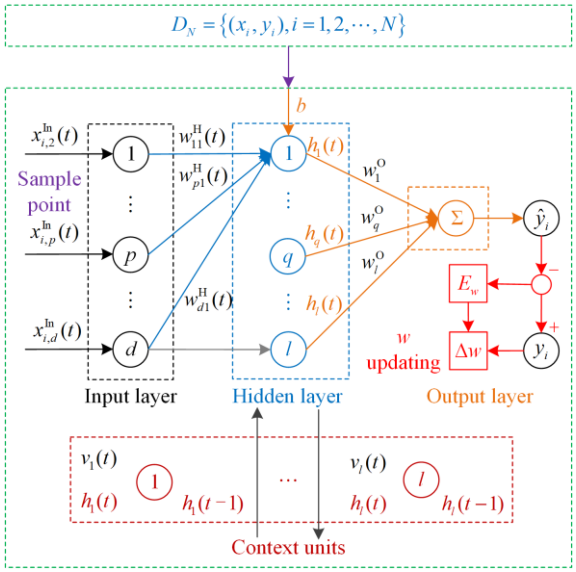

Fig. 13. Architecture of the ENN modeling method.

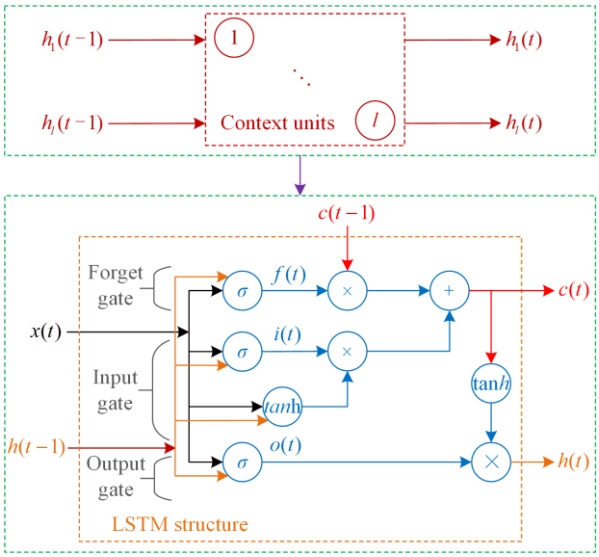

Fig. 14. Structure of the LSTM network.

As can be seen from Fig. 14, the structure of LSTM comprises three essential gates: the input, the forget, and the output. They are used to activate functions and filter information through neurons [129], [140]. During the internal state update, the input gate filters incoming information, while the forget gate discards redundant information. Finally, the output and new hidden layers are computed via the output gate.

B. EIS-CS-ENN-based Estimation Framework

As a traditional RNN, the ENN is often directly used to estimate the battery health state in specific conditions. For example, in [141], the HIs related to the life degradation of LIBs are extracted, and the relationship between HIs and health state is analyzed by the grey relation analysis (GRA) method. Finally, the extracted HIs are regarded as the ENN input to estimate the health state.

Given the novel methods proposed in some recent papers, the superiority of ENN is no longer obvious. In [142], a bat method-extreme learning machine (BA-ELM) model is established for estimation. Five error metrics and three kinds of diagrams are provided to evaluate the estimation results between the ENN and BA-ELM models. The results demonstrate that the evaluation function of the BA-ELM model converges faster, while yielding smaller RMSE and MAE values. Therefore, it is urgently required to improve ENN or integrate other methods based on ENN for state estimation.

Based on the accuracy improvement requirement of ENN-based health state estimation methods, reference [127] improves a data-driven model based on the fusion of autoregressive moving average (ARMA) and ENN. The test results indicate that, compared with the ARMA and ENN, the proposed fusion method significantly improves the estimated outcomes according to the metric values. However, this method is a fusion method and does not improve the structure of the ENN, and does not have any optimization for the ENN model itself. Hence, a method based on EIS-CS-ENN is proposed. This method has the ability to overcome the shortcomings of low estimation accuracy and poor applicability in variable temperature environments.

Specifically, the ENN is optimized using the CS method. Then, 19 features extracted from the EIS method are input into the CS-ENN model for training and testing. The features are reduced to four principal components as the final input samples. Finally, the trained CS-ENN health state estimation model is used to obtain accurate estimation results. In the capacity test, reference [143] completes the impedance measurement of 60 frequency points with 10 frequency points per decade from 20 MHz to 20 kHz, including 120 dimensions in each sample. The dimensions consist of 60 real component data $x_{\mathrm{re}}(i)$ and 60 imaginary component data $x_{\mathrm{im}}(i)$. Since the EIS method can characterize battery degradation to a certain extent, the EIS variance of each degradation cycle is selected as the first HI, shown as:

$$\begin{cases} J_1 = \dfrac{(x_{\mathrm{re}}(1)-M)^2+\cdots+(x_{\mathrm{re}}(60)-M)^2}{120} + \\ \qquad \dfrac{(x_{\mathrm{im}}(1)-M)^2+\cdots+(x_{\mathrm{im}}(60)-M)^2}{120} \\ M = \dfrac{x_{\mathrm{re}}(1)+\cdots+x_{\mathrm{re}}(60)+x_{\mathrm{im}}(1)+\cdots+x_{\mathrm{im}}(60)}{120} \end{cases} \tag{2}$$

where M is the mean value of each sample and J_1 represents the value of the first HI. According to the internal electrochemical mechanism of LIBs, EIS includes high-frequency, middle-frequency, and low-frequency parts [35], [144]. By plotting the EIS and Nyquist cycle diagram of the LIBs with the increase of cycle number at 35 °C and 100% SOC, it is found that 0.2 Hz, 2.16 Hz, and 17.80 Hz in the low-frequency part are more suitable

to be used as HIs to estimate health state than other frequencies. Furthermore, the study reveals a clear linear relationship between the size of imaginary components and the number of cycles [145]. With the cycle number increasing, the 20 Hz of the high-frequency part is similar to the three low-frequency features, although the transformation trend is not as obvious as in the low-frequency features. Therefore, the slope, concavity-convexity, and coordinates of the above four points are taken as the 2nd to 17th HIs, and their calculation formulas are shown as:

$$\begin{cases} J_2, J_3 = \dfrac{x_{\text{im}}(i+1) - x_{\text{im}}(i-1)}{x_{\text{re}}(i+1) - x_{\text{re}}(i-1)}, (i = 31, \cdots, 40) \\ J_4 = \dfrac{x_{\text{im}}(2) - x_{\text{im}}(1)}{x_{\text{re}}(2) - x_{\text{re}}(1)} \\ J_5 = \dfrac{x_{\text{im}}(60) - x_{\text{im}}(59)}{x_{\text{re}}(60) - x_{\text{re}}(59)} \\ J_6 = \dfrac{J_2(31+1) - J_2(31-1)}{x_{\text{re}}(31+1) - x_{\text{re}}(31-1)} \\ J_7 = \dfrac{J_3(40+1) - J_3(40-1)}{x_{\text{re}}(40+1) - x_{\text{re}}(40-1)} \\ J_8 = \dfrac{J_4(2) - J_4(1)}{x_{\text{re}}(2) - x_{\text{re}}(1)} \\ J_9 = \dfrac{J_5(60) - J_5(59)}{x_{\text{re}}(60) - x_{\text{re}}(59)} \\ J_i = x_{\text{im}}(1), x_{\text{re}}(1), x_{\text{im}}(31), (i = 10,11,12) \\ J_i = x_{\text{re}}(31), x_{\text{im}}(40), x_{\text{re}}(40), (i = 13,14,15) \\ J_i = x_{\text{im}}(60), x_{\text{re}}(60), (i = 16,17) \end{cases} \tag{3}$$

where J_i represents the ith HI.

To study the slight changes of EIS with the increase of cycles, kurtosis and skewness coefficients are introduced as the 18th and 19th HIs to quantify data anomaly and skewness, respectively, shown as:

$$\begin{cases} J_{18} = \dfrac{(1/60)\sum_{i=1}^{60}\left[(x_{\text{re}}(i) - M) + (x_{\text{im}}(i) - M)\right]^3}{(1/59)\sum_{i=1}^{60}\left[(x_{\text{re}}(i) - M) + (x_{\text{im}}(i) - M)^2\right]^{3/2}} \\ J_{19} = \dfrac{(1/60)\sum_{i=1}^{60}\left[(x_{\text{re}}(i) - M) + (x_{\text{im}}(i) - M)\right]^4}{(1/59)\sum_{i=1}^{60}\left[(x_{\text{re}}(i) - M) + (x_{\text{im}}(i) - M)^2\right]^2} \end{cases} \tag{4}$$

The classification and extraction of HIs are shown in Fig. 15.

The max-min normalization method is introduced to deal with HIs to avoid the computational issues caused by dimensional inconsistency. The idea of GRA is incorporated to establish the correlation and mapping relationship between HIs and capacity degradation. GRA is rooted in the fundamental concept of comparing the degree of similarity in curves between reference and comparison sequences. The steps for calculating the relational degree are shown in Table III.

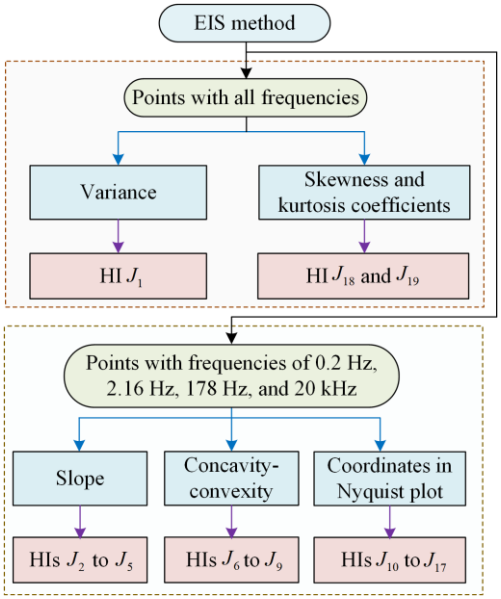

Fig. 15. Classification and extraction of HIs.

TABLE III
CALCULATION PROCESS OF THE GRA METHOD

Steps	Process
Step 1	Search and determine reference and comparison sequences. Expressions of sequences are shown in (5).
Step 2	After dimensionless processing of the sequences, the relational coefficient between the sequences is calculated, as shown in (6).
Step 3	Calculate the relational degree between the sequences, as shown in (7).

$$\begin{cases} X_i = \left\{x_i(k) \middle| k = 1,2,\cdots,n\right\} \\ Y = \left\{y(k) \middle| k = 1,2,\cdots,n\right\} \end{cases} \tag{5}$$

$$\begin{cases} \xi_i(k) = \dfrac{\min\limits_i \min\limits_k \Delta_i(k) + \rho \min\limits_i \min\limits_k \Delta_i(k)}{\Delta_i(k) + \rho \min\limits_i \min\limits_k \Delta_i(k)} \\ \Delta_i(k) = \left| y(k) - x_i(k) \right| \end{cases} \tag{6}$$

$$r_i = \frac{1}{n}\sum_{i=1}^{n} \xi_i(k), (k = 1,2,\cdots,n) \tag{7}$$

where X and Y represent the reference and comparison sequences; i is the serial number of the comparison sequence; k indicates the sequence number of each time point in the sequence; n represents the sequence length; x denotes a certain value in the sequence; ξ is the relational coefficient at each point; ρ means the resolution coefficient; and r denotes the relational degree. The closer the relationship degree is to 1, the closer the relationship between HIs and battery degradation is.

Although the change trends of the above 19 HIs are different, they all have strong relationships with the health state. These results illustrate that EIS is directly related to the intrinsic reaction of battery degradation. However, the slope and concavity-convexity of the point at 2.16 Hz and the concavity-convexity of the points at 0.2 Hz, 7.8 Hz, and 20 Hz are lower than those

of other HIs. After filtering out the five HIs, the principal component analysis (PCA) method is used to reduce the number of input HIs and the amount of computation. In the PCA method, the cumulative variance contribution rate is set to 85%, and the maximum value of the eigenvectors is selected to obtain the dimensionality-reduced eigenmatrix. The PCA analysis results show that the sum of the contribution rates of the four principal components exceeds 85%, so it is appropriate to use the feature data of the four principal components to represent most of the original data. As a basic RNN, ENN is often used for data training and testing, and its specific structure has been described in detail in Subsection A of Section II. The nonlinear state-space equation of the ENN is shown as:

$$\begin{cases} y(k) = g(\omega_3 x(k)) \\ x(k) = f(\omega_1 x_c(k) + \omega_2 (u(k-1))) \\ x_c(k) = x(k-1) \end{cases} \tag{8}$$

where y is the output of the output layer; x is the output of the hidden layer; u is the input of the input layer; x_c is the output of a context layer; ω_3, ω_2, and ω_1 represent the corresponding weight matrices between the output, hidden, input, and context layers, respectively; $g(\cdot)$ denotes the transfer function of the output neuron; and $f(\cdot)$ indicates the transfer function of the hidden layer neurons.

The CS method is adopted to optimize the initial weights and thresholds of ENN to make up for the defect of ENN in the local optimization function. By controlling the population size and probability, the CS method can maintain the balance between local search and diversity so that the search results can avoid local optimality and converge to the optimal global solution. The specific steps to optimize ENN using the CS method are shown in Table IV.

TABLE IV
SPECIFIC STEPS FOR OPTIMIZING ENN USING THE CS METHOD

Steps	Process
Step 1	Build ENN and initialize CS parameters.
Step 2	Take the ENN parameters as the initial quantity and iteratively update each parameter.
Step 3	The optimal parameters are selected according to fitness. If the results meet the requirements, go to Step 5; if not, go to Step 4.
Step 4	Iteratively update the parameters to build a new solution for the next generation, and then return to Step 3.
Step 5	At the end of the cycle, the optimal results of CS are taken as the initial weight and threshold of ENN.

First, the ENN parameters are constructed and initialized. Then, the number of nodes in the input, output, and optimal hidden layers are obtained from the training data. Finally, the initial parameters of ENN are optimized by CS to continuously train the network to obtain the best health state results. The flowchart of the health state estimation method based on the CS-ENN model proposed in this paper is shown in Fig. 16.

To critically evaluate the estimation performance of the models, MaxE ($E_{1,k}$), MAE ($E_{2,k}$), RMSE ($E_{3,k}$), and coefficient of determination (R^2) are introduced as evaluation metrics, given as:

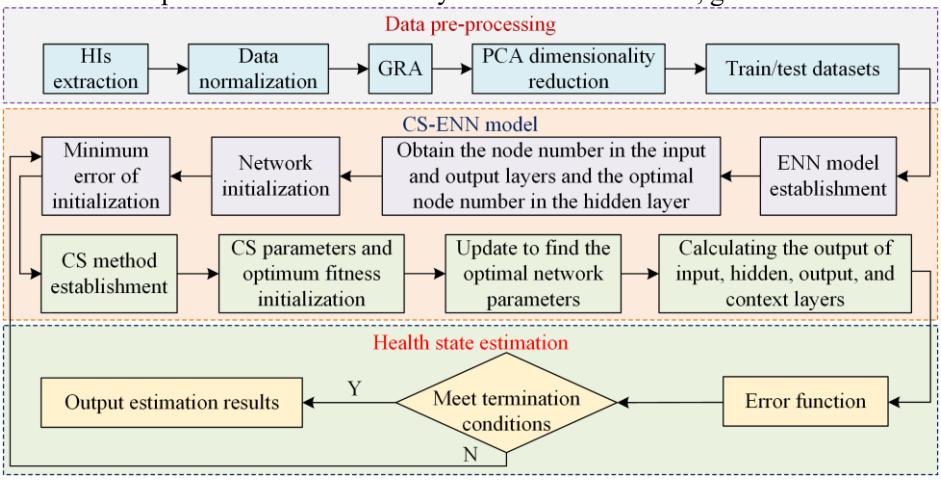

Fig. 16. Flowchart of the health state estimation method based on the CS-ENN model.

$$\begin{cases} E_{1,k} = \max 1,2,\cdots,N \left| y_k - \hat{y}_k \right| \\ E_{2,k} = \dfrac{1}{N} \sum_{k=1}^{N} \left| y_k - \hat{y}_k \right| \\ E_{3,k} = \sqrt{\dfrac{1}{N} \sum_{k=1}^{N} (y_k - \hat{y}_k)^2} \\ R^2_{\ k} = 1 - \dfrac{\sum_{k=1}^{N} (y_k - \hat{y}_k)^2}{\sum_{k=1}^{N} (y_k - \bar{y})^2} \end{cases} \tag{9}$$

where N is the total sample steps; y_k and $\hat{y}_k$ are the actual and estimated health state values at time point k, respectively; while $\bar{y}$ is the average value of the actual state value at time point k. The estimation results of ENN, ELM, SVM, BPNN, and CS-ENN with different datasets are compared in multi-temperature conditions. The estimation results of different HIs as the CS-ENN input are also compared.

C. Application Analysis from Other Literature

In addition to the EIS-CS-ENN-based method described in detail in Subsection B of Section II, other ANN-based methods are also widely used. For example, for the FFNN model in ANN, reference [146] extracts appropriate HIs and training data through large data analysis, and proposes a framework for intelligent battery health state estimation based on the capacity estimation model of the FFNN. In [96], part of the IC curve is smoothed through a Gaussian filter, while [131] develops an improved FFNN model that can simulate the battery voltage charging characteristics to smooth the IC curve. Reference [131] also points out that since the nodes of the proposed FFNN have a certain physical meaning and also change with capacity, this model is significant in estimating the health state.

For the CNN model in ANN, reference [138] proposes, for the first time, an online capacity estimation scheme for LIBs based on a deep convolutional neural network (DCNN). This approach proposes a DCNN model for estimating the capacity of individual cells based on voltage, current, and capacity measurements obtained during multiple charging cycles. Causal convolution is used to process the time series data, rather than standard convolution. However, the use of causal convolution results in a deeper network, which slows down training and increases memory usage.

To solve these problems, reference [147] uses a dilated convolution, which skips the input during convolution. Specifically, a battery health state estimation method is developed to separate global capacity degradation and local capacity regeneration based on a temporal convolutional network (TCN) and empirical mode decomposition (EMD). Causal convolution and dilated convolution are introduced into the model to improve the ability to capture local capacity regeneration. In addition, in this method, dilated convolution can also solve the problems of memory increase and training slowdown caused by causal convolution when processing temporal data. The overall system framework for battery health diagnosis is shown in Fig. 17.

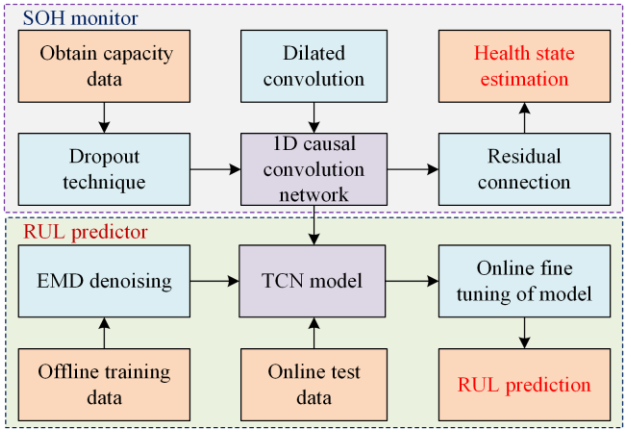

Fig. 17. System framework for health diagnosis based on TCN and EMD.

For the basic RNN model in an ANN, reference [65] develops a joint estimation method for capacity and SOC. In the SOC online estimation part, the method is based on ECM, RLS, and AEKF, whereas in the capacity estimation part, the method is based on the relationship between the voltage curve and battery degradation, using ENN to obtain an accurate battery health state for correcting the SOC. In [127], a health state estimation method is proposed for LIBs based on ARMA and ENN. Specifically, after selecting the HIs related to degradation, EMD is used to preprocess the original capacity degradation data and eliminate the phenomenon of capacity regeneration. The ARMA and ENN models are constructed using time series data and residual data.

When using the LSTM model in RNN to estimate the battery health state, two aspects have been studied: optimizing HIs and optimizing the network architecture. For example, reference [148] optimizes HIs based on GRA and entropy weight methods and inputs the optimized HIs into the LSTM model, based on the LSTM structure diagram shown in Fig. 14. The battery health state estimation flowchart is established as shown in Fig. 18.

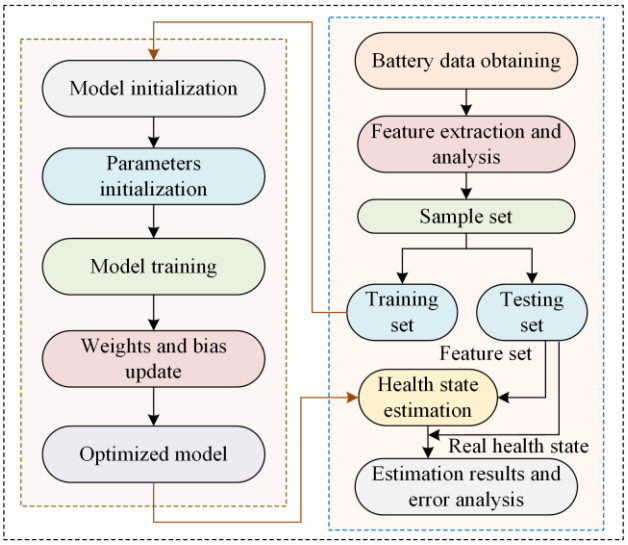

Fig. 18. Battery health state estimation flowchart based on LSTM network.

Reference [149] optimizes HIs using the locally weighted linear regression (LWLR) method and the maximum information coefficient (MIC). The LSTM network is used to learn more of the nonlinear degraded relationship between capacity and HIs. In [150], external characteristic parameters are extracted as the HIs, and neighborhood component analysis (NCA) is adopted to eliminate redundant information about the HIs. Additionally, this study proposes a differential evolution grey wolf optimizer (DEGWO) to address the issue of hyperparameter selection in LSTM models. The DEGWO is used to optimize hyperparameters for enhanced model performance. Reference [151] constructs

and compares the normal RNN [152], LSTM [98], [153], gated recurrent unit neural network (GRUNN) [154], opposite bidirectional structure [155] and other neural network models. The results demonstrate that the LSTM and the bidirectional LSTM (Bi-LSTM) have higher versatility and accuracy in estimating battery health states. In summary, the ANN-based methods have become key tools for massive data analysis in energy storage systems, and the greatest challenges are the efficiency and accuracy of the ANN model training process [156]–[158].

IV. Comparative Analysis of Health State Effects Using Different ANN Methods

Currently, it is most popular to use ANN-based methods to obtain the health state. ANN-based methods do not require data preprocessing or understanding of the principles and structure of LIBs. In addition, there is no need to establish a physical model, and the estimation is accurate with massive data. However, the disadvantages of the ANN-based model are that they require high efficiency of methods, high frequency and accuracy of data, and high dependence on data transmission. It is a trend to monitor the battery state in the future by implanting ANN-based methods into the BMS of energy storage systems. With the wide application of cloud computing, cloud storage, big data, and other emerging technologies, the status of ANN-based methods is becoming more significant. Different ANN-based methods have different effects on estimating battery health state, and it is necessary to discuss the research directions and future trends of health state estimation approaches [159], [160].

By introducing some evaluation indicators, the results of ANN-based models across the literature are compared and analyzed to find the most appropriate method to estimate the health state in different conditions. The accuracy of state estimation depends on the reliability of the initial parameters of the model [14], [161]. Using the RMSE, MaxE, and MAE as evaluation indicators, the estimation effects of different ANN-based methods under different HIs are compared, as shown in Table V.

By comparing and analyzing the data from Table V, it can be seen that the ANN-based methods are effective and accurate. BPNN and ENN, as the most basic FFNN and RNN models, respectively, have the worst performance in various evaluation metrics, and this can be blamed on their simple structure. Models such as EIS-CS-ENN, LSTM, Bi-LSTM, DCNN and GRUNN are more complex in structure, and this complexity results in more accurate estimation. It is worth noting that, compared with LSTM, GRUNN has fewer parameters and faster convergence. Correspondingly, without a more complex structure, GRUNN cannot consider past observations during training like LSTM. The comprehensive evaluation results of the EIS-CS-ENN model are the best. When different HIs are used as the input to the same ANN model, the evaluation results are different. This conclusion can be obtained from the evaluation indicators of the two ENN models in Table V. This also verifies that HIs are critical for model training and testing.

TABLE V
Estimation Effects of Different ANN-based Methods Under Different HIs

ANN methods	HIs	RMSE	MaxE	MAE
BPNN [95]	Parameters of the first-order ECM		7.2%	<5%
ENN [142]	Charging: constant current time, constant voltage time, and voltage change; Discharging: total time, temperature change, and voltage change	3.075%		2.0936 %
EIS-CS-ENN [143]	Four principal components consisting of fourteen EIS features	0.74%		0.53%
ENN [143]	Same as CS-ENN	1.74%		1.64%
LSTM [151]	Constant current time, constant voltage time, constant current time proportion, constant voltage time proportion, and total charge time	0.762%		0.652%
Bi-LSTM [151]	Same as LSTM	0.743%		0.678%
DCNN [138]	Voltage, current, and charge capacity during partial charge cycles	0.302%	2.491%	
GRUNN [154]	Six HIs are extracted from the differential temperature curves		2.28%	

Data from laboratory tests spanning over a year throughout the whole life cycle is conveniently accessible at the following URLs: https://www.researchgate.net/project/Battery-life-test and https://www.researchgate.net/project/Whole-Life-Cycle-Test.

V. Conclusion

As the key pieces of equipment in energy storage systems, LIBs provide safe and green energy, but the accurate estimation of their health state to ensure the reliable operation of systems is difficult, and has been the recent focus of research. This paper introduces the classification of battery health state methods and elucidates the current status, applications, and prospects of related estimation methods from different perspectives and as described in the literature. The advantages and disadvantages of different estimation methods and the improving direction are then analyzed, compared, and reviewed. The results show that the data-driven and

hybrid methods are suited to massive data and difficult physical modeling conditions. The data-driven ANN-based method has advantages of non-parametric characteristics and strong computing power, and is suitable for most engineering environments, meets the requirements of accurate estimation, and provides an effective battery state acquisition scheme. Therefore, this paper focuses on the ANN model in the data-driven estimation method and selects an EIS-CS-ENN model from the literature related to the ANN model for detailed process description and calculation framework establishment. Specifically, the EIS-CS-ENN-based health state estimation method is a hybrid of direct measurement and data-driven methods. The 14 features in EIS are selected to form 4 principal components, and are used as inputs to the CS-ENN model for data training and testing. In addition, the application of ANN-based methods proposed in other literature is analyzed. Finally, this review assesses and compares the estimation performance of various ANN models using several evaluation metrics and HIs. The results indicate that the four types of ANN models can significantly improve estimation accuracy and modeling adaptability. The evaluation results of the EIS-CS-ENN model are the best.

Future work will focus on the review of the health state estimation methods for LIB packs and the estimation or prediction methods of battery states for effective real-time BMS applications. Specifically, the following research areas are proposed:

1) To study various states of battery packs, improved battery pack models with different connection methods should be further established.

2) Because of the requirement of effective real-time BMS applications, further research should be conducted on health state estimation methods that are not affected by internal electrochemical reactions.

3) For application to the estimation and prediction of multiple battery states, data-driven technologies such as data mining and a cloud computing platform need to be developed.

ACKNOWLEDGMENT

Not applicable.

AUTHORS' CONTRIBUTIONS

Ran Xiong: full-text writing, revised writing and investigation. Shunli Wang: revised writing and the construction of the paper framework. Paul Takyi-Aninakwa: revised writing. Siyu Jin: supervision. Carlos Fernandez: visualization. Qi Huang: investigation. Weihao Hu: revised writing and investigation. Wei Zhan: revised writing. All authors read and approved the final manuscript.

FUNDING

This work is supported by the National Natural Science Foundation of China (No. 62173281 and No. 61801407), the Sichuan Science and Technology Program (No. 2019YFG0427 and No. 2023YFG0108), the China Scholarship Council (No. 201908515099), and the Fund of Robot Technology used for the Special Environment Key Laboratory of Sichuan Province (No. 18kftk03).

AVAILABILITY OF DATA AND MATERIALS

Please contact the corresponding author for data material request.

DECLARATIONS

Competing interests: The authors declare that they have no known competing financial interests or personal relationships that could have appeared to influence the work reported in this article.

AUTHORS' INFORMATION

Ran Xiong received the B.S. and M.S. degrees from the School of Information Engineering, Southwest University of Science and Technology, Mianyang, China. He is now with the School of Mechanical and Electrical Engineering, University of Electronic Science and Technology of China, Chengdu, China. His research interests include lithium-ion battery state estimation and new power system optimization.

Shunli Wang received the M.S. and Ph.D. degrees from the School of Information Engineering, Southwest University of Science and Technology, Mianyang, China. He is currently a professor with the Southwest University of Science and Technology. He is currently an authoritative expert of the new energy research field and the leader of New Energy Measurement and Control Research Team.

Paul Takyi-Aninakwa received the B.S. degree in Mechanical Engineering from Kwame Nkrumah University of Science and Technology, Ghana, from 2011 to 2015. He then pursued his M.S. in Mechanical Engineering at the Southwest University of Science and Technology, China, from 2019 to 2021. Currently, he is a final year Ph.D. student in Control Science and Engineering at the Southwest University of Science and Technology, China, and is set to graduate in 2024. His research interests mainly include the simulation and characterization of energy storage systems, artificial intelligence, and state modeling and estimation of lithium-ion batteries.

Siyu Jin received the M.S. degree in electrical engineering and automation from Northeastern University, Shenyang, China, in 2019. She is currently pursuing the

Ph.D. degree with the Department of AAU Energy, Aalborg University (AAU), Aalborg, Denmark. Her current research interests include battery state estimation and battery management systems.

Carlos Fernandez received the Ph.D. degree in Electrocatalytic Reactions from the University of Hull and then worked as a consultant technologist in Hull and in a post-doctoral position in Manchester. He is currently a senior lecturer at Robert Gordon University, Scotland. His research interests include analytical chemistry, sensors and materials, and renewable energy.

Qi Huang is currently a professor with the Southwest University of Science and Technology (SWUST), Mianyang, China, and the University of Electronic Science and Technology of China, Chengdu, China. He is the president of SWUST and the director with the Sichuan State Provincial Laboratory of Power System Wide-Area Measurement and Control, Chengdu. His current research and academic interests include power system instrumentation, power system monitoring and control, and informatics for smart electric energy systems.

Weihao Hu received the B.Eng. and M.Sc. degrees in electrical engineering from Xi'an Jiaotong University, Xi'an, China, in 2004 and 2007, respectively, and the Ph.D. degree from Aalborg University, Aalborg, Denmark, in 2012. He is currently a full professor with the School of Mechanical and Electrical Engineering, University of Electronic Science and Technology of China, Chengdu, China. His research interests include intelligent energy systems and renewable power generation.

Wei Zhan is currently a senior investigator with the SPIC Southwest Energy Research Institute, Chengdu, China. His current research and interests include power system instrumentation, power system monitoring and control, future distributed energy and new energy economy.

REFERENCES

[1] Z. Yi, Z. Chen, and K. Yin *et al*., "Sensing as the key to the safety and sustainability of new energy storage devices," *Protection and Control of Modern Power Systems*, vol. 8, no. 2, pp. 1-22, Apr. 2023.

[2] N. Yang, X. Zhang, and B. Shang *et al.*, "Unbalanced discharging and aging due to temperature differences among the cells in a lithium-ion battery pack with parallel combination," *Journal of Power Sources*, vol. 306, no. 29, pp. 733-741, Feb. 2016.

[3] L. Adua, "Reviewing the complexity of energy behavior: Technologies, analytical traditions, and household energy consumption data in the United States," *Energy Research & Social Science*, vol. 59, no. 1, Jan. 2020.

[4] X. Chen, L. Huang, and J. Liu *et al.*, "Peak shaving benefit assessment considering the joint operation of nuclear and battery energy storage power stations: Hainan case study," *Energy*, vol. 239, no. 1, pp. 1-15, Jan. 2022.

[5] A. Z. Shaqsi, K. Sopian, and A. Al-Hinai, "Review of energy storage services, applications, limitations, and benefits," *Energy Reports*, vol. 6, no. 7, pp. 288-306, Dec. 2020.

[6] Y. Jin, Z. Zhao, and S. Miao *et al.*, "Explosion hazards study of grid-scale lithium-ion battery energy storage station," *Journal of Energy Storage*, vol. 42, no. 10, pp. 102987-102998, Oct. 2021.

[7] A. G. Olabi, "Renewable energy and energy storage systems," *Energy*, vol. 136, no. 10, pp. 1-6, Oct. 2017.

[8] U. Akram, M. Nadarajah, and R. Shah *et al.*, "A review on rapid responsive energy storage technologies for frequency regulation in modern power systems," *Renewable and Sustainable Energy Reviews*, vol. 120, no. 3, pp. 109626-109638, Mar. 2020.

[9] R. Zalosh, P. Gandhi, and A. Barowy, "Lithium-ion energy storage battery explosion incidents," *Journal of Loss Prevention in the Process Industries*, vol. 72, no. 9, pp. 104560-104571, Sept. 2021.

[10] E. Bullich-Massagué, F. J. Cifuentes-García, and I. Glenny-Crende *et al*., "A review of energy storage technologies for large scale photovoltaic power plants," *Applied Energy*, vol. 274, no. 15, pp. 115213-115224, Sept. 2020.

[11] F. Eroglu, M. Kurtoglu, and A. M. Vural, "Bidirectional DC-DC converter based multilevel battery storage systems for electric vehicle and large-scale grid applications: a critical review considering different topologies, state-of-charge balancing and future trends," *IET Renewable Power Generation*, vol. 15, no. 5, pp. 915-938, Feb. 2021.

[12] J. Figgener, P. Stenzel, and K. P. Kairies *et al*., "The development of stationary battery storage systems in Germany-status 2020," *Journal of Energy Storage*, vol. 33, no. 9, pp. 101982-101994, Jan. 2021.

[13] Q. Xiao, Y. Jin, and H. Jia *et al.*, "Review of fault diagnosis and fault-tolerant control methods of the modular multilevel converter under submodule failure," *IEEE Transactions on Power Electronics*, vol. 38, no. 10, pp. 12059-12077, Jun. 2023.

[14] S. Wang, P. Ren, and P. Takyi-Aninakwa *et al.*, "A critical review of improved deep convolutional neural network for multi-timescale state prediction of lithium-ion batteries," *Energies*, vol. 15, no. 14, pp. 5053-5072, Jul. 2022.

[15] N. Wassiliadis, J. Adermann, and A. Frericks *et al*., "Revisiting the dual extended Kalman filter for battery state-of-charge and state-of-health estimation: a use-case life cycle analysis," *Journal of Energy Storage*, vol. 19, no. 10, pp. 73-87, Oct. 2018.

[16] Y. Luo, P. Qi, and Y. Kan *et al*., "State of charge estimation method based on the extended Kalman filter algorithm with consideration of time-varying battery parameters," *International Journal of Energy Research*, vol. 44, no. 13, pp. 10538-10550, Jul. 2020.

[17] X. Hu, K. Zhang, and K. Liu *et al*., "Advanced fault diagnosis for lithium-ion battery systems: a review of fault mechanisms, fault features, and diagnosis proce-

dures," *IEEE Industrial Electronics Magazine*, vol. 14, no. 3, pp. 65-91, Sept. 2020.

[18] L. Xu, Z. Deng, and X. Hu, "Battery health estimation using electrochemical aging model and ensemble Kalman filtering," in *2021 IEEE International Future Energy Electronics Conference*, Taiwan, China, Nov. 2021, pp.1-6.

[19] X. Tan, D. Zhan, and P. Lyu *et al*., "Online state-of-health estimation of lithium-ion battery based on dynamic parameter identification at multi timescale and support vector regression," *Journal of Power Sources*, vol. 484, no. 1, pp. 1-10, Feb. 2021.

[20] Y. Sun, X. Hao, and M. Pecht *et al*., "Remaining useful life prediction for lithium-ion batteries based on an integrated health indicator," *Microelectronics Reliability*, vol. 88, no. 9, pp. 1189-1194, Sept. 2018.

[21] B. O. Kang, M. Lee, and Y. Kim *et al*., "Economic analysis of a customer-installed energy storage system for both self-saving operation and demand response program participation in South Korea," *Renewable and Sustainable Energy Reviews*, vol. 94, no. 10, pp. 69-83, Oct. 2018.

[22] H. Tian, P. Qin, and K. Li *et al*., "A review of the state of health for lithium-ion batteries: research status and suggestions," *Journal of Cleaner Production*, vol. 261, no. 10, pp. 120813-120821, Jul. 2020.

[23] M. S. H. Lipu, M. A. Hannan, and A. Hussain *et al*., "A review of state of health and remaining useful life estimation methods for lithium-ion battery in electric vehicles: challenges and recommendations," *Journal of Cleaner Production*, vol. 205, no. 20, pp. 115-133, Dec. 2018.

[24] R. Xiong, S. Wang, and C. Fernandez *et al*., "A novel joint estimation method of state of charge and state of health based on the strong tracking-dual adaptive extended Kalman filter algorithm for the electric vehicle lithium-ion batteries," *International Journal of Electrochemical Science*, vol. 16, no. 11, pp. 1-32, Nov. 2021.

[25] C. Jiang, S. Wang, and B. Wu *et al*., "A state-of-charge estimation method of the power lithium-ion battery in complex conditions based on adaptive square root extended Kalman filter," *Energy*, vol. 219, no. 15, pp. 119603-119624, Mar. 2021.

[26] M. Lucu, E. Martinez-Laserna, and I. Gandiaga *et al*., "A critical review on self-adaptive Li-ion battery ageing models," *Journal of Power Sources*, vol. 401, no. 15, pp. 85-101, Oct. 2018.

[27] J. Meng, L. Cai, and G. Luo *et al*., "Lithium-ion battery state of health estimation with short-term current pulse test and support vector machine," *Microelectronics Reliability*, vol. 88-90, no. 9, pp. 1216-1220, Sept. 2018.

[28] J. Zhang, P. Wang, and Q. Gong *et al*., "SOH estimation of lithium-ion batteries based on least squares support vector machine error compensation model," *Journal of Power Electronics*, vol. 21, no. 11, pp. 1712-1723, Sept. 2021.

[29] R. Xiong, L. Li, and J. Tian, "Towards a smarter battery management system: a critical review on battery state of health monitoring methods," *Journal of Power Sources*, vol. 405, no. 30, pp. 18-29, Nov. 2018.

[30] Y. Li, K. Liu, and A. M. Foley *et al*., "Data-driven health estimation and lifetime prediction of lithium-ion batteries: a review," *Renewable and Sustainable Energy Reviews*, vol. 113, no. 10, pp. 109254-109264, Oct. 2019.

[31] H. Ren, Y. Zhao, and S. Chen *et al*., "Design and implementation of a battery management system with active charge balance based on the SOC and SOH online estimation," *Energy*, vol. 166, no. 1, pp. 908-917, Jan. 2019.

[32] P. Takyi-Aninakwa, S. Wang, and H. Zhang *et al*., "An optimized relevant long short-term memory-squared gain extended Kalman filter for the state of charge estimation of lithium-ion batteries," *Energy*, vol. 260, pp. 1-15, Dec. 2022.

[33] M. Ge, Y. Liu, and X. Jiang *et al*., "A review on state of health estimations and remaining useful life prognostics of lithium-ion batteries," *Measurement*, vol. 174, no. 4, pp. 109057-109064, Apr. 2021.

[34] A. Basia, Z. Simeu-Abazi, and E. Gascard *et al*., "Review on state of health estimation methodologies for lithium-ion batteries in the context of circular economy," *CIRP Journal of Manufacturing Science and Technology*, vol. 32, no. 9, pp. 517-528, Jan. 2021.

[35] S. Yang, C. Zhang, and J. Jiang *et al*., "Review on state-of-health of lithium-ion batteries: Characterizations, estimations and applications," *Journal of Cleaner Production*, vol. 314, no. 10, pp. 128015-128024, Sept. 2021.

[36] G. K. Prasad and C. D. Rahn, "Model based identification of aging parameters in lithium ion batteries," *Journal of Power Sources*, vol. 232, no. 15, pp. 79-85, Jun. 2013.

[37] X. Han, L. Lu, and Y. Zheng *et al*., "A review on the key issues of the lithium ion battery degradation among the whole life cycle," *eTransportation*, vol. 1, no. 8, pp. 100005-100014, Aug. 2019.

[38] D. Chen, C. Tao, and T. Chen *et al*., "Pomegranate-like Silicon-based anodes self-assembled by hollow-structured Si/void@C nanoparticles for Li-ion batteries with high performances," *Nanotechnology*, vol. 32, no. 9, pp. 1-9, Dec. 2020.

[39] Y. Hua, A. Cordoba-Arenas, and N. Warner *et al*., "A multi time-scale state-of-charge and state-of-health estimation framework using nonlinear predictive filter for lithium-ion battery pack with passive balance control," *Journal of Power Sources*, vol. 280, no. 15, pp. 293-312, Apr. 2015.

[40] W. Diao, J. Jiang, and C. Zhang *et al*., "Energy state of health estimation for battery packs based on the degradation and inconsistency," *Energy Procedia*, vol. 142, no. 11, pp. 3578-3583, Dec. 2017.

[41] S. Zhang, X. Guo, and X. Dou *et al*., "A rapid online calculation method for state of health of lithium-ion battery based on coulomb counting method and differential voltage analysis," *Journal of Power Sources*, vol. 479, no. 15, pp. 228740-228749, Dec. 2020.

[42] C. R. Lashway and O. A. Mohammed, "Adaptive battery management and parameter estimation through physics-based modeling and experimental verification," *IEEE Transactions on Transportation Electrification*, vol. 2, no. 4, pp. 454-464, Apr. 2016.

[43] S. Wang, X. Xiong, and C. Zou *et al*., "An improved coulomb counting method based on dual open-circuit

voltage and real-time evaluation of battery dischargeable capacity considering temperature and battery aging," *International Journal of Energy Research*, vol. 45, no. 12, pp. 17609-17621, Jul. 2021.

[44] S. E. Li, B. Wang, and H. Peng *et al*., "An electrochemistry-based impedance model for lithium-ion batteries," *Journal of Power Sources*, vol. 258, no. 1, pp. 9-18, Jul. 2014.

[45] U. Westerhoff, T. Kroker, and K. Kurbach *et al*., "Electrochemical impedance spectroscopy based estimation of the state of charge of lithium-ion batteries," *Journal of Energy Storage*, vol. 8, no. 9, pp. 244-256, Nov. 2016.

[46] S. Yoon, I. Hwang, and C. W. Lee *et al*., "Power capability analysis in lithium ion batteries using electrochemical impedance spectroscopy," *Journal of Electroanalytical Chemistry*, vol. 655, no. 1, pp. 32-38, May 2011.

[47] Y.-H. Chiang, W.-Y. Sean, and J.-C. Ke, "Online estimation of internal resistance and open-circuit voltage of lithium-ion batteries in electric vehicles," *Journal of Power Sources*, vol. 196, no. 8, pp. 3921-3932, Apr. 2011.

[48] Z. Wei, A. Salehi, and G. Lin *et al*., "Probing Li-ion concentration in an operating lithium ion battery using in situ Raman spectroscopy," *Journal of Power Sources*, vol. 449, no. 15, pp. 227361-227370, Feb. 2020.

[49] M. J. Mühlbauer, A. Schökel, and M. Etter *et al*., "Probing chemical heterogeneity of Li-ion batteries by in operando high energy X-ray diffraction radiography," *Journal of Power Sources*, vol. 403, no. 1, pp. 49-55, Nov. 2018.

[50] T. Tsuda, A. Imanishi, and T. Sano *et al*., "In situ electron microscopy and X-ray photoelectron spectroscopy for high capacity anodes in next-generation ionic liquid-based Li batteries," *Electrochimica Acta*, vol. 279, no. 1, pp. 1-10, Jul. 2018.

[51] X. Ding, D. Zhang, and J. Cheng *et al*., "An improved Thevenin model of lithium-ion battery with high accuracy for electric vehicles," *Applied Energy*, vol. 254, no. 15, pp. 113615-113621, Nov. 2019.

[52] N. Tian, Y. Wang, and J. Chen *et al*., "One-shot parameter identification of the Thevenin's model for batteries: methods and validation," *Journal of Energy Storage*, vol. 29, no. 6, pp. 101282-101289, Jun. 2020.

[53] M. Zeng, P. Zhang, and Y. Yang *et al*., "SOC and SOH joint estimation of the power batteries based on fuzzy unscented kalman filtering algorithm," *Energies*, vol. 12, no. 16, pp. 3122-3131, Aug. 2019.

[54] Y. He, Q. Li, and X. Zheng *et al*., "Equivalent hysteresis model based SOC estimation with variable parameters considering temperature," *Journal of Power Electronics*, vol. 21, no. 3, pp. 590-602, Feb. 2021.

[55] Z. Deng, L. Yang, and Y. Cai *et al*., "Online available capacity prediction and state of charge estimation based on advanced data-driven algorithms for lithium iron phosphate battery," *Energy*, vol. 112, no. 1, pp. 469-480, Oct. 2016.

[56] F. Baronti, N. Femia, and R. Saletti *et al*., "Preisach modelling of lithium-iron-phosphate battery hysteresis," *Journal of Energy Storage*, vol. 4, no. 12, pp. 51-61, Dec. 2015.

[57] C. Liu, M. Hu, and G. Jin *et al*., "State of power estimation of lithium-ion battery based on fractional-order equivalent circuit model," *Journal of Energy Storage*, vol. 41, no. 9, pp. 102954-102967, Sept. 2021.

[58] Q. Zhang, Y. Shang, and Y. Li *et al*., "A novel fractional variable-order equivalent circuit model and parameter identification of electric vehicle Li-ion batteries," *ISA Transactions*, vol. 97, no. 2, pp. 448-457, Feb. 2020.

[59] G. Jin, L. Li, and Y. Xu *et al*., "Comparison of SOC estimation between the integer-order model and fractional-order model under different operating conditions," *Energies*, vol. 13, no. 7, pp. 1785-1797, Apr. 2020.

[60] X. Hu, S. Li, and H. Peng, "A comparative study of equivalent circuit models for Li-ion batteries," *Journal of Power Sources*, vol. 198, no. 15, pp. 359-367, Jan. 2012.

[61] T. Feng, L. Yang, and X. Zhao *et al*., "Online identification of lithium-ion battery parameters based on an improved equivalent-circuit model and its implementation on battery state-of-power prediction," *Journal of Power Sources*, vol. 281, no. 1, pp. 192-203, May 2015.

[62] E. Rijanto, L. Rozaqi, and A. Nugroho *et al*., "RLS with optimum multiple adaptive forgetting factors for SOC and SOH estimation of Li-ion battery," in *2017 5th International Conference on Instrumentation, Control, and Automation*, Yogyakarta, Indonesia, Aug. 2017, pp. 73-77.

[63] J. Shi, H. Guo, and D. Chen, "Parameter identification method for lithium-ion batteries based on recursive least square with sliding window difference forgetting factor," *Journal of Energy Storage*, vol. 44, no. 15, pp. 103485-103494, Dec. 2021.

[64] L. Fang, J. Li, and B. Peng, "Online estimation and error analysis of both SOC and SOH of lithium-ion battery based on DEKF method," *Energy Procedia*, vol. 158, no. 1, pp. 3008-3013, Feb. 2019.

[65] X. Li, Z. Wang, and L. Zhang, "Co-estimation of capacity and state-of-charge for lithium-ion batteries in electric vehicles," *Energy*, vol. 174, no. 1, pp. 33-44, May 2019.

[66] R. Xiong, Y. Zhang, H. He *et al*., "A double-scale, particle-filtering, energy state prediction algorithm for lithium-ion batteries," *IEEE Transactions on Industrial Electronics*, vol. 65, no. 2, pp. 1526-1538, Feb. 2018.

[67] J. Qiao, S. Wang, and C. Yu *et al*., "A novel bias compensation recursive least square-multiple weighted dual extended Kalman filtering method for accurate state-of-charge and state-of-health co-estimation of lithium-ion batteries," *International Journal of Circuit Theory and Applications*, vol. 49, no. 11, pp. 3879-3893, Aug. 2021.

[68] L. Ma, Y. Xu, and H. Zhang *et al*., "Co-estimation of state of charge and state of health for lithium-ion batteries based on fractional-order model with multi-innovations unscented Kalman filter method," *Journal of Energy Storage*, vol. 52, no. 15, pp. 104904-104912, Aug. 2022.

[69] J. Bi, T. Zhang, and H. Yu *et al*., "State-of-health estimation of lithium-ion battery packs in electric vehicles based on genetic resampling particle filter," *Applied Energy*, vol. 182, no. 15, pp. 558-568, Nov. 2016.

[70] M. Doyle, T. F. Fuller, and J. Newman, "Modeling of galvanostatic charge and discharge of the lithium/polymer/insertion cell," *Journal of The Electrochemical Society*, vol. 140, no. 6, pp. 1526-1539, Jun. 1993.

[71] M. Shen and Q. Gao, "A review on battery management system from the modeling efforts to its multiapplication and integration," *International Journal of Energy Research*, vol. 43, no. 10, pp. 5042-5075, Apr. 2019.

[72] Y. Wang, J. Tian, and Z. Sun *et al*., "A comprehensive review of battery modeling and state estimation approaches for advanced battery management systems," *Renewable and Sustainable Energy Reviews*, vol. 131, no. 1, pp. 110015-110024, Oct. 2020.

[73] Y. Zhao, P. Stein, and Y. Bai *et al*., "A review on modeling of electro-chemo-mechanics in lithium-ion batteries," *Journal of Power Sources*, vol. 413, no. 15, pp. 259-283, Feb. 2019.

[74] X. Zhang, Y. Gao, and B. Guo *et al*., "A novel quantitative electrochemical aging model considering side reactions for lithium-ion batteries," *Electrochimica Acta*, vol. 343, no. 20, pp. 136070-136081, May 2020.

[75] J. L. Lee, A. Chemistruck, and G. L. Plett, "One-dimensional physics-based reduced-order model of lithium-ion dynamics," *Journal of Power Sources*, vol. 220, no. 15, pp. 430-448, Dec. 2012.

[76] J. L. Lee, L. L. Aldrich, and K. D. Stetzel *et al*., "Extended operating range for reduced-order model of lithium-ion cells," *Journal of Power Sources*, vol. 255, no. 1, pp. 85-100, Jun. 2014.

[77] Z. Deng, L. Yang, and H. Deng *et al*., "Polynomial approximation pseudo-two-dimensional battery model for online application in embedded battery management system," *Energy,* vol. 142, no. 1, pp. 838-850, Jan. 2018.

[78] L. Ren, G. Zhu, and J. Kang *et al*., "An algorithm for state of charge estimation based on a single-particle model," *Journal of Energy Storage*, vol. 39, no. 7, pp. 102644-102651, Jul. 2021.

[79] X. Han, M. Ouyang, and L. Lu *et al*., "Simplification of physics-based electrochemical model for lithium ion battery on electric vehicle, Part II: pseudo-two-dimensional model simplification and state of charge estimation," *Journal of Power Sources*, vol. 278, no. 15, pp. 814-825, Mar. 2015.

[80] J. Li, K. Adewuyi, and N. Lotfi *et al*., "A single particle model with chemical/mechanical degradation physics for lithium ion battery state of health (SOH) estimation," *Applied Energy*, vol. 212, no. 15, pp. 1178-1190, Feb. 2018.

[81] R. Mehta and A. Gupta, "An improved single-particle model with electrolyte dynamics for high current applications of lithium-ion cells," *Electrochimica Acta*, vol. 389, no. 1, pp. 138623-138631, Sept. 2021.

[82] N. Lotfi, J. Li and R. G. Landers *et al*., "Li-ion battery state of health estimation based on an improved single particle model," in *2017 American Control Conference*, Seattle, USA, May 2017, pp. 86-91.

[83] T. R. B. Grandjean, L. Li, and M. X. Odio *et al*., "Global sensitivity analysis of the single particle lithium-ion battery model with electrolyte," in *2019 IEEE Vehicle Power and Propulsion Conference*, Hanoi, Vietnam, Oct. 2019, pp. 1-7.

[84] K. K. Sadabadi, X. Jin, and G. Rizzoni, "Prediction of remaining useful life for a composite electrode lithium ion battery cell using an electrochemical model to estimate the state of health," *Journal of Power Sources*, vol. 481, no. 1, pp. 228861-228871, Jan. 2021.

[85] L. Zheng, L. Zhang, and J. Zhu *et al*., "Co-estimation of state-of-charge, capacity and resistance for lithium-ion batteries based on a high-fidelity electrochemical model," *Applied Energy*, vol. 180, no. 15, pp. 424-434, Oct. 2016.

[86] C. Zou, C. Manzie, and D. Nešić *et al*., "Multi-time-scale observer design for state-of-charge and state-of-health of a lithium-ion battery," *Journal of Power Sources*, vol. 335, no. 15, pp. 121-130, Dec. 2016.

[87] A. Bartlett, J. Marcicki, and S. Onori *et al*., "Model-based state of charge estimation and observability analysis of a composite electrode lithium-ion battery," in *52nd IEEE Conference on Decision and Control*, Firenze, Italy, Dec. 2013, pp. 7791-7796.

[88] S. J. Moura, M. Krstic, and N. A. Chaturvedi, "Adaptive PDE observer for battery SOC/SOH estimation," in *ASME 2012 5th Annual Dynamic Systems and Control Conference joint with the JSME 2012 11th Motion and Vibration Conference*, Fort Lauderdale, USA, Oct. 2012, pp. 101-110.

[89] Z. Wu, L. Yin, and R. Xiong *et al*., "A novel state of health estimation of lithium-ion battery energy storage system based on linear decreasing weight-particle swarm optimization algorithm and incremental capacity-differential voltage method," *International Journal of Electrochemical Science*, vol. 17, no. 7, pp. 1-32, Jul. 2022.

[90] M. Zhang, D. Yang, and J. Du *et al*., "A review of SOH prediction of Li-ion batteries based on data-driven algorithms," *Energies*, vol. 16, no. 7, pp. 3167-3178, Mar. 2023.

[91] T. Oji, Y. Zhou, and S. Ci *et al*., "Data-driven methods for battery SOH estimation: Survey and a critical analysis," *IEEE ACCESS*, vol. 9, no. 1, pp. 126903-126916, Sept. 2021.

[92] A. Eddahech, O. Briat, and N. Bertrand *et al*., "Behavior and state-of-health monitoring of Li-ion batteries using impedance spectroscopy and recurrent neural networks," *International Journal of Electrical Power and Energy Systems*, vol. 42, no. 1, pp. 487-494, Nov. 2012.

[93] G. W. You, S. Park, and D. Oh, "Real-time state-of-health estimation for electric vehicle batteries: A data-driven approach," *Applied Energy*, vol. 176, no. 15, pp. 92-103, Aug. 2016.

[94] H. Pan, Z. Lv, and H. Wang *et al*., "Novel battery state-of-health online estimation method using multiple health indicators and an extreme learning machine," *Energy*, vol. 160, no. 1, pp. 466-477, Oct. 2018.

[95] D. Yang, Y. Wang, and R. Pan *et al*., "A neural network based state-of-health estimation of lithium-ion battery in electric vehicles," *Energy Procedia*, vol. 105, no. 5, pp. 2059-2064, May 2017.

[96] S. Zhang, B. Zhai, and X. Guo *et al*., "Synchronous estimation of state of health and remaining useful lifetime for lithium-ion battery using the incremental capacity and artificial neural networks," *Journal of Energy Storage*, vol. 26, no. 12, pp. 100951-100961, Dec. 2019.

[97] W. Zhang, X. Li, and X. Li, "Deep learning-based prognostic approach for lithium-ion batteries with adaptive time-series prediction and on-line validation," *Measurement*, vol. 164, no. 11, pp. 108052-108061, Nov. 2020.

[98] P. Li, Z. Zhang, and Q. Xiong *et al*., "State-of-health estimation and remaining useful life prediction for the lithium-ion battery based on a variant long short term memory neural network," *Journal of Power Sources*, vol. 459, no. 31, pp. 228069-228078, May 2020.

[99] J. C. A. Anton, P. J. G. Nieto, and C. B. Viejo *et al*., "Support vector machines used to estimate the battery state of charge," *IEEE Transactions on Power Electronics*, vol. 28, no. 12, pp. 5919-5926, Jan. 2013.

[100] M. A. Hannan, M. S. H. Lipu, and A. Hussain *et al*., "A review of lithium-ion battery state of charge estimation and management system in electric vehicle applications: Challenges and recommendations," *Renewable and Sustainable Energy Reviews*, vol. 78, no. 10, pp. 834-854, Oct. 2017.

[101] G. Mountrakis, J. Im, and C. Ogole, "Support vector machines in remote sensing: a review," *ISPRS Journal of Photogrammetry and Remote Sensing*, vol. 66, no. 3, pp. 247-259, May 2011.

[102] I. S. Han and C. B. Chung, "Performance prediction and analysis of a PEM fuel cell operating on pure oxygen using data-driven models: a comparison of artificial neural network and support vector machine," *International Journal of Hydrogen Energy*, vol. 41, no. 24, pp. 10202-10211, Jun. 2016.

[103] A. Nuhic, T. Terzimehic, and T. Soczka-Guth *et al*., "Health diagnosis and remaining useful life prognostics of lithium-ion batteries using data-driven methods," *Journal of Power Sources*, vol. 239, no. 1, pp. 680-688, Oct. 2013.

[104] T. Qin, S. Zeng, and J. Guo, "Robust prognostics for state of health estimation of lithium-ion batteries based on an improved PSO–SVR model," *Microelectronics Reliability*, vol. 55, no. 9-10, pp. 1280-1284, Sept. 2015.

[105] H. Li, D. Pan, and C. L. P. Chen, "Intelligent prognostics for battery health monitoring using the mean entropy and relevance vector machine," *IEEE Transactions on Systems, Man, and Cybernetics: Systems*, vol. 44, no. 7, pp. 851-862, Feb. 2014.

[106] D. Wang, Q. Miao, and M. Pecht, "Prognostics of lithium-ion batteries based on relevance vectors and a conditional three-parameter capacity degradation model," *Journal of Power Sources*, vol. 239, no. 1, pp. 253-264, Oct. 2013.

[107] X. Qin, Q. Zhao, and H. Zhao *et al*., "Prognostics of remaining useful life for lithium-ion batteries based on a feature vector selection and relevance vector machine approach," in *2017 IEEE International Conference on Prognostics and Health Management*, Dallas, USA, Jun. 2017, pp. 1-6.

[108] L. Wei, X. Yan, and F. Xue *et al*., "Optimal fuzzy logic control of energy storage systems for V/f support in distribution networks considering battery degradation," *International Journal of Electrical Power and Energy Systems*, vol. 139, no. 7, pp. 107867-107875, Jul. 2022.

[109] W. Pan, Q. Chen, and M. Zhu *et al*., "A data-driven fuzzy information granulation approach for battery state of health forecasting," *Journal of Power Sources*, vol. 475, no. 1, pp. 228716-228724, Nov. 2020.

[110] M. Landi and G. Gross, "Measurement techniques for online battery state of health estimation in vehicle-to-grid applications," *IEEE Transactions on Instrumentation and Measurement*, vol. 63, no. 5, pp. 1224-1234, Jan. 2014.

[111] J. Tian, R. Xiong, and W. Shen, "State-of-health estimation based on differential temperature for lithium ion batteries," *IEEE Transactions on Power Electronics*, vol. 35, no. 10, pp. 10363-10373, Mar. 2020.

[112] Y. Zhang, Y. Liu, and J. Wang *et al*., "State-of-health estimation for lithium-ion batteries by combining model-based incremental capacity analysis with support vector regression," *Energy*, vol. 239, no. 15, pp. 121986-121995, Jan. 2022.

[113] M. Dubarry, B. Y. Liaw, and M. S. Chen *et al*., "Identifying battery aging mechanisms in large format Li ion cells," *Journal of Power Sources*, vol. 196, no. 7, pp. 3420-3425, Apr. 2011.

[114] M. Maures, A. Capitaine, and J. Y. Delétage *et al*., "Lithium-ion battery SoH estimation based on incremental capacity peak tracking at several current levels for online application," *Microelectronics Reliability*, vol. 114, no. 11, pp. 113798-113805, Nov. 2020.

[115] P. Keil, S.F. Schuster, and J. Wilhelm *et al*., "Calendar aging of lithium-ion batteries I. Impact of the graphite anode on capacity fade," *Journal of the Electrochemical Society*, vol. 163, no. 9, pp. 1872-1884, Jul. 2016.

[116] X. Han, M. Ouyang, and L. Lu *et al*., "A comparative study of commercial lithium ion battery cycle life in electrical vehicle: Aging mechanism identification," *Journal of Power Sources*, vol. 251, no. 1, pp. 38-54, Apr. 2014.

[117] Y. Li, M. Abdel-Monem, and R. Gopalakrishnan *et al*., "A quick on-line state of health estimation method for Li-ion battery with incremental capacity curves processed by Gaussian filter," *Journal of Power Sources*, vol. 373, no. 1, pp. 40-53, Jan. 2018.

[118] A. Naha, S. Han, and S. Agarwal *et al*., "An incremental voltage difference based technique for online state of health estimation of Li-ion batteries," *Scientific reports*, vol. 10, no. 1, pp. 9526-9534, Jun. 2020.

[119] M. Berecibar, M. Garmendia, and I. Gandiaga *et al*., "State of health estimation algorithm of LiFePO4 battery packs based on differential voltage curves for battery management system application," *Energy*, vol. 103, no. 1, pp. 784-796, May 2016.

[120] R. Xiong, J. Tian, and H. Mu *et al*., "A systematic model-based degradation behavior recognition and health monitoring method for lithium-ion batteries," *Applied Energy*, vol. 207, no. 1, pp. 372-383, Dec. 2017.

[121] A. Zenati, P. Desprez, and H. Razik, "Estimation of the SOC and the SOH of li-ion batteries, by combining impedance measurements with the fuzzy logic inference," in *IECON 2010-36th Annual Conference on*

IEEE Industrial Electronics Society, Glendale, USA, Nov. 2010, pp. 1773-1778.

[122]M. J. Esfandyari, M. R. H. Yazdi, and V. Esfahanian *et al*., "A hybrid model predictive and fuzzy logic based control method for state of power estimation of series-connected Lithium-ion batteries in HEVs," *Journal of Energy Storage*, vol. 24, no. 8, pp. 100758-100769, Aug. 2019.

[123]J. Park, M. Lee, and G. Kim *et al*., "Integrated approach based on dual extended Kalman filter and multivariate autoregressive model for predicting battery capacity using health indicator and SOC/SOH," *Energies*, vol. 13, no. 9, pp. 2138-2150, Apr. 2020.

[124]S. Son, S. Jeong, and E. Kwak *et al*., "Integrated framework for SOH estimation of lithium-ion batteries using multiphysics features," *Energy*, vol. 238, no. 1, pp. 121712-121721, Jan. 2022.

[125]Z. Chu, M. S. Trimboli, and G. L. Plett *et al*., "A control-oriented electrochemical model for lithium-ion battery, Part I: lumped-parameter reduced-order model with constant phase element," *Journal of Energy Storage*, vol. 25, no. 10, pp. 100828-100839, Oct. 2019.

[126]G. Liu, X. Zhang, and Z. Liu, "State of health estimation of power batteries based on multi-feature fusion models using stacking algorithm," *Energy*, vol. 259, no. 15, pp. 124851-124865, Nov. 2022.

[127]Z. Chen, Q. Xue, and R. Xiao *et al*., "State of health estimation for lithium-ion batteries based on fusion of autoregressive moving average model and Elman neural network," *IEEE Access*, vol. 7, no. 1, pp. 102662-102678, Jul. 2019.

[128]K. Liu, K. Li, and Q. Peng *et al*., "Data-driven hybrid internal temperature estimation approach for battery thermal management," *Complexity*, vol. 2018, no. 1, pp. 1-15, Jul. 2018.

[129]X. Sui, S. He, and S. B. Vilsen *et al*., "A review of non-probabilistic machine learning-based state of health estimation techniques for lithium-ion battery," *Applied Energy*, vol. 300, no. 15, pp. 117346-117357, Oct. 2021.

[130]M. Cao, T. Zhang, and B. Yu *et al*., "A method for interval prediction of satellite battery state of health based on sample entropy," *IEEE Access*, vol. 7, no. 1, pp. 141549-141561, Sep. 2019.

[131]X. Han, X. Feng, and M. Ouyang *et al*., "A comparative study of charging voltage curve analysis and state of health estimation of lithium-ion batteries in electric vehicle," *Automotive Innovation*, vol. 2, no. 2, pp. 263-275, Dec. 2019.

[132]P. Zhou, Z. He, and T. Han *et al*., "A rapid classification method of the retired LiCoxNiyMn1−x−yO2 batteries for electric vehicles," *Energy Reports*, vol. 6, no. 11, pp. 672-683, Nov. 2020.

[133]Q. Yang, J. Xu, and X. Li *et al*., "State-of-health estimation of lithium-ion battery based on fractional impedance model and interval capacity," *International Journal of Electrical Power and Energy Systems*, vol. 119, no. 7, pp. 105883-105894, Jul. 2020.

[134]A. Bonfitto, "A method for the combined estimation of battery state of charge and state of health based on artificial neural networks," *Energies*, vol. 13, no. 10, pp. 2548-2560, May 2020.

[135]J. Tian, R. Xiong, and W. Shen, *et al*., "Flexible battery state of health and state of charge estimation using partial charging data and deep learning," *Energy Storage Materials*, vol. 51, no. 10, pp. 372-381, Oct. 2022.

[136]L. Ungurean, M. V. Micea, and G. Cârstoiu, "Online state of health prediction method for lithium-ion batteries, based on gated recurrent unit neural networks," *International Journal of Energy Research*, vol. 44, no. 8, pp. 6767-6777, Apr. 2020.

[137]P. Khumprom and N. Yodo, "A data-driven predictive prognostic model for lithium-ion batteries based on a deep learning algorithm," *Energies*, vol. 12, no. 4, pp. 660-669, Feb. 2019.

[138]S. Shen, M. Sadoughi, and X. Chen *et al*., "A deep learning method for online capacity estimation of lithium-ion batteries," *Journal of Energy Storage*, vol. 25, no. 10, pp. 100817-100825, Oct. 2019.

[139]N. Ma, H. Yin, and K. Wang, "Prediction of the remaining useful life of supercapacitors at different temperatures based on improved long short-term memory," *Energies*, vol. 16, no. 14, pp. 5240-5251, Jul. 2023.

[140]G.-W. You, S. Park, and D. Oh, "Diagnosis of electric vehicle batteries using recurrent neural networks," *IEEE Transactions on Industrial Electronics*, vol. 64, no. 6, pp. 4885-4893, Feb. 2017.

[141]Z. Cheng, Q. Xue, and Y. Liu *et al*., "State of health estimation for lithium-ion batteries based on Elman neural network," *DEStech Transactions on Environment Energy and Earth Science*, vol. 1, no. 1, pp. 1-10, Oct. 2019.

[142]D. Ge, Z. Zhang, and X. Kong *et al*., "Extreme learning machine using bat optimization algorithm for estimating state of health of lithium-ion batteries," *Applied Sciences*, vol. 12, no. 3, pp. 1398-1407, Jan. 2022.

[143]C. Chang, S. Wang, and J. Jiang *et al*., "Lithium-ion battery state of health estimation based on electrochemical impedance spectroscopy and cuckoo search algorithm optimized Elman neural network," *Journal of Electrochemical Energy Conversion and Storage*, vol. 19, no. 3, pp. 30912-30922, Apr. 2022.

[144]A. Eddahech, O. Briat, and J. M. Vinassa, "Performance comparison of four lithium–ion battery technologies under calendar aging," *Energy*, vol. 84, no. 1, pp. 542-550, May 2015.

[145]Y. Zhang, Q. Tang, and Y. Zhang *et al*., "Identifying degradation patterns of lithium ion batteries from impedance spectroscopy using machine learning," *Nature communications*, vol. 11, no. 1, pp. 1706-1718, Apr. 2020.

[146]L. Song, K. Zhang, and T. Liang *et al*., "Intelligent state of health estimation for lithium-ion battery pack based on big data analysis," *Journal of Energy Storage*, vol. 32, no. 12, pp. 101836-101848, Dec. 2020.

[147]D. Zhou, Z. Li, and J. Zhu *et al*., "State of health monitoring and remaining useful life prediction of lithium-ion batteries based on temporal convolutional network," *IEEE Access*, vol. 8, no. 1, pp. 53307-53320, Mar. 2020.

[148]Y. Wu, Q. Xue, and J. Shen *et al*., "State of health estimation for lithium-ion batteries based on healthy features and long short-term memory," *IEEE Access*, vol. 8, no. 1, pp. 28533-28547, Feb. 2020.

[149]Z. He, X. Shen, and Y. Sun *et al*., "State-of-health estimation based on real data of electric vehicles concerning user behavior," *Journal of Energy Storage*, vol. 41, no. 9, pp. 102867-102877, Sept. 2021.

[150]Y. Ma, C. Shan, and J. Gao *et al*., "A novel method for state of health estimation of lithium-ion batteries based on improved LSTM and health indicators extraction," *Energy*, vol. 251, no. 1, pp. 123973-123984, Jul. 2022.

[151]K. Li, Y. Wang, and Z. Chen, "A comparative study of battery state-of-health estimation based on empirical mode decomposition and neural network," *Journal of Energy Storage*, vol. 54, no. 10, pp. 105333-105348, Oct. 2022.

[152]H. Chaoui and C.C. Ibe-Ekeocha, "State of charge and state of health estimation for lithium batteries using recurrent neural networks," *IEEE Transactions on Vehicular Technology*, vol. 66, no. 10, pp. 8773-8783, Jun. 2017.

[153]Y. Ma, C. Shan, and J. Gao *et al*., "Multiple health indicators fusion-based health prognostic for lithium-ion battery using transfer learning and hybrid deep learning method," *Reliability Engineering & System Safety*, vol. 229, no. 1, pp. 108818-108828, Jan. 2023.

[154]Z. Chen, H. Zhao, and Y. Zhang *et al*., "State of health estimation for lithium-ion batteries based on temperature prediction and gated recurrent unit neural network," *Journal of Power Sources*, vol. 521, no. 15, pp. 230892-230904, Feb. 2022.

[155]F. K. Wang, Z. E. Amogne, J. H. Chou *et al*., "Online remaining useful life prediction of lithium-ion batteries using bidirectional long short-term memory with attention mechanism," *Energy*, vol. 254, no. 5, pp. 124344-124354, Sept. 2022.

[156]A. G. Kashkooli, H. Fathiannasab, and Z. Mao *et al*., "Application of artificial intelligence to state-of-charge and state-of-health estimation of calendar-aged lithium-ion pouch cells," *Journal of the Electrochemical Society*, vol. 166, no. 4, pp. 605-614, Feb. 2019.

[157]J. Yue, X. Xia, and C. Lv *et al.*, "Research on the prediction of state of health and remaining useful life of lithium-ion batteries considering the amount of health factors information," *Power System Protection and Control*, vol. 51, no. 22, pp. 74-87, Nov. 2023. (in Chinese)

[158]Y. Guo, D. Yang, and Y. Zhang *et al*., "Online estimation of SOH for lithium-ion battery based on SSA-Elman neural network," *Protection and Control of Modern Power Systems*, vol. 7, no. 3, pp. 1-17, Oct. 2022.

[159]S. Wang, S. Jin, and D. Bai *et al*., "A critical review of improved deep learning methods for the remaining useful life prediction of lithium-ion batteries," *Energy Reports*, vol. 7, no. 1, pp. 5562-5574, Nov. 2021.

[160]Y. Liu, L. Wang, and D. Li *et al*., "State-of-health estimation of lithium-ion batteries based on electrochemical impedance spectroscopy: a review," *Protection and Control of Modern Power Systems*, vol. 8, no. 3, pp. 1-17, Jul. 2023.

[161]L. Mao, J. Wen, and J. Zhao *et al*., "Joint estimation of SOC and SOH at lithium-ion battery charging cut-off voltage based on an ensemble extreme learning machine," *Power System Protection and Control*, vol. 51, no. 11, pp. 86-95, Jun. 2023. (in Chinese)